Available online at www.sciencedirect.com
SCIENCE DIRECT
Lithos 89 (2006) 24–46
LITHOS
www.elsevier.com/locate/lithos

Serpentinization and dehydration in the upper mantle beneath Fuerteventura (eastern Canary Islands): Evidence from mantle xenoliths

M.A. Abu El-Rus [1], E.-R. Neumann *, V. Peters

Physics of Geological Processes, University of Oslo, PO Box 1048 Blindern, N-0316 Oslo, Norway

Received 16 September 2004; accepted 5 September 2005
Available online 9 November 2005

Abstract

Mantle xenoliths from Fuerteventura (spinel-bearing harzburgites, dunites, and rare lherzolites and wehrlites) in the easternmost part of the Canary Islands chain, are highly deformed and show a wide range in textures from protogranular and porphyroclastic with olivine and orthopyroxene porphyroclasts, to rocks with "fibrous textures" (no orthopyroxene porphyroclasts, large, porous clusters of fibrous orthopyroxene, olivine porphyroclasts criss-crossed by stringy trails of fibrous orthopyroxene and fluid inclusions). The whole group of xenoliths covers a wider compositional range (e.g. $Fo_{86.6–92.7}$, 0.18–0.44 wt.% NiO, and up to 0.25 wt.% CaO in olivine; <0.01–2.5 wt.% TiO_2 and 0.7–5.5 wt.% Al_2O_3 in clinopyroxenes in harzburgites and lherzolites, and relatively Ti–Fe^{3+}-rich spinels in some rocks). Rocks with orthopyroxene porphyroclasts cover a restricted compositional range typical of depleted oceanic peridotites (e.g. $Fo_{90.7–91.4}$, 0.36–0.41 wt.% NiO, and <0.10 wt.% CaO in cores of olivine porphyroclasts; ≤0.12 wt.% TiO_2, 1.0–1.8 wt.% Al_2O_3 in clinopyroxene; low Ti and Fe^{3+}, and high Cr in spinel). These rocks are interpreted as pieces of the highly refractory oceanic lithosphere that accreted to the oldest oceanic crust in this part of the Atlantic Ocean, later modified by different processes. This mantle was highly depleted due to melt extraction, and had a composition similar to that of the most refractory peridotites collected along the Mid-Atlantic Ridge. Also the oceanic mantle beneath the other Canary Islands appears to have had similar composition before the onset of the Canary Islands magmatism. The "fibrous textures" in many xenoliths from Fuerteventura are interpreted as the results of partial serpentinization, later followed by heating and dehydration during the formation of Fuerteventura. The Fuerteventura magmatism has also caused metasomatism and reactions in the lithospheric mantle beneath Fuerteventura, leading to decreased Si and increased Fe+Ca+Na±Ti.

Keywords: Canary Island; Petrogenesis; Serpentinization; Dehydration; Metasomatism

1. Introduction

Detailed studies of mantle xenoliths from the islands of La Palma, Hierro, Tenerife and Lanzarote in the Canary Islands archipelago (Fig. 1) have given a lot of information about the origin and evolution of the upper mantle beneath the Canary Islands (e.g. Neumann, 1991; Siena et al., 1991; Neumann et al., 1995, 2002, 2004; Wulff-Pedersen et al., 1996). Recently we

* Corresponding author.
E-mail addresses: aliabualrus@yahoo.com (M.A. Abu El-Rus), e.r.neumann@geo.uio.no (E.-R. Neumann).
[1] Present address: Geology Department, Assiut University, Assiut 71516, Egypt.

0024-4937/$ - see front matter © 2005 Elsevier B.V. All rights reserved.
doi:10.1016/j.lithos.2005.09.005

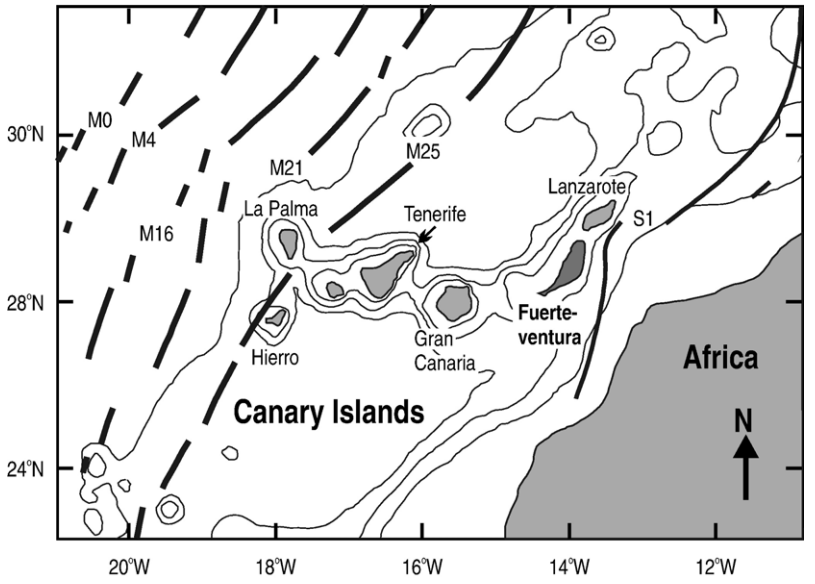

Fig. 1. Map of the Canary Islands showing bathymetry (with 1000 m contours) and magnetic anomalies (simplified after Verhoef et al., 1991 and Roest et al., 1992).

have found mantle xenoliths from Fuerteventura in the easternmost part of the Canary Islands chain that exhibit some unusual textures. Similar textures have been observed in rare xenoliths from Lanzarote, also in the easternmost part of the Canary Islands chain, but have not been found in any of the central and western islands. These textures, which include domains of fibrous orthopyroxene and indications of partial breakdown of olivine, suggest that the upper mantle beneath the easternmost Canary Islands may have been subjected to local serpentinization followed by prograde metamorphism and dehydration. Alternatively, these textures may result from reactions between the peridotite wall-rock and an infiltrating fluid. The extent of serpentinization in the oceanic upper mantle is a topic of considerable speculation (e.g. Minshull et al., 1998; Whitmarsh et al., 2001; Schroeder et al., 2002). To our knowledge evidence of serpentinization has not before been reported from ocean islands. It is the aim of this study (a) to report the textural variations of the mantle xenoliths from Fuerteventura and the compositional variations that accompany the different textural types, and (b) to unravel the processes that led to the observed textural and compositional variations.

2. Geological setting

The Canary Islands consist of seven large islands that form a roughly east–west trending islands chain located between 100 and 500 km from the coast of western Africa (Fig. 1). The islands are located on oceanic lithosphere ranging from ≈180 Ma in the east to ≈150 Ma in the west (e.g. Verhoef et al., 1991; Roest et al., 1992; Hoernle, 1998). Subaerial lavas in the Canary Islands show a crude westwards decrease in age from ≈24 Ma in Fuerteventura, to ≈1.1 Ma in Hierro (e.g. Abdel-Monem et al., 1971, 1972; Schmincke, 1982; Balogh et al., 1999).

Fuerteventura is the second largest of the Canary Islands (Fig. 1). Its oldest part is made up by the Basal Complex (≥64 to about 22 Ma; e.g. Stillman, 1987; Balogh et al., 1999) which comprises large ultramafic and mafic intrusions, syenites, basaltic dyke swarms, submarine volcanic rocks, deep-water sediments, submarine volcanic rocks, and plutonic intrusions (e.g. Fúster et al., 1968; Stillman et al., 1975; Le Bas et al., 1986; Coello et al., 1992). The Basal Complex is intruded by carbonatites, syenite dykes and ijolites, 22–21 Ma old (e.g. Le Bas et al., 1986; Balogh et al., 1999). The Basal Complex is overlain by a basaltic shield complex formed in the period from ca. 23 to ca. 13 Ma (e.g. Fúster et al., 1968; Coello et al., 1992). Then followed a long volcanic hiatus before the post-erosional cycle which started ca. 5 Ma ago and appears to have continued into Holocene time (e.g. Fúster et al., 1968; Coello et al., 1992).

3. Petrography

The mantle xenoliths of this study were collected from two Holocene volcano cones in northern Fuerteventura, west of the town Corralejo. The localities are termed FBA1 and FT9. The host lavas are basanites.

The xenoliths are up to 15 cm in diameter, are generally fresh and have sub-angular to rounded shapes. Interaction with the host basalts appears only to have affected the outermost rims of the xenoliths.

The most common rock types are spinel harzburgite and spinel dunite; spinel lherzolites are less abundant and wehrlite is rare. No significant differences in the xenolith populations were observed between the two localities. The xenoliths belong to the Cr-diopside group of Wilshire and Shervais (1975) or Group I of Frey and Prinz (1978). The mineral assemblage is olivine (ol) and orthopyroxene (opx; rare or absent in dunites), minor amounts of Cr-spinel (sp), and minor amounts of Cr-diopside (cpx). Most xenoliths exhibit protogranular to porphyroclastic textures (Mercier and Nicolas, 1975), a few are granular and fine-grained. The protogranular to porphyroclastic samples show different modes of appearance of orthopyroxene (porphyroclasts or fibrous aggregates) and olivine (well-defined porphyroclasts or porphyroclasts with mottled rims and numerous stringy fluid inclusion trails). On the basis of their textural characteristics the xenoliths have been divided into a series of groups which are described below.

Because many xenoliths contain fine-grained fibrous domains where it is very difficult to distinguish olivine and clinopyroxene from orthopyroxene, classification is based on qualitative assessments of the proportions of olivine, orthopyroxene and clinopyroxene, together with SiO_2 and CaO concentrations: spinel harzburgites have $SiO_2 > 41$ wt.% and CaO < 1.5 wt.%; lherzolites have CaO > 2.0 wt.%, dunites have $SiO_2 < 41$ wt.% and CaO < 1.5 wt.% (Fig. 2).

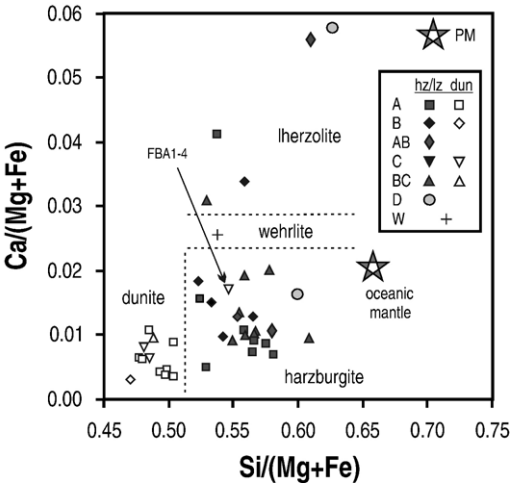

Fig. 2. Rock classification based on petrography and the relationship between the atomic ratios Si/(Mg+Fe) and Ca/(Mg+Fe). Ratios Si/(Mg+Fe*) > 0.5 (the ratio for olivine) are caused by the presence of spinel.

3.1. Group A xenoliths

Group A is the largest group and comprises spinel harzburgites, rare lherzolites, and spinel dunites. These xenoliths are protogranular to porphyroclastic and consist of ol ± opx porphyroclasts, and ol + sp ± opx ± cpx neoblasts. All grain boundaries are well-defined; fibrous domains and mottled rims on olivine are lacking or rare (Fig. 3a). The porphyroclasts are highly strained; some samples exhibit foliation. Fluid inclusion trails are common.

Olivine forms strongly strained, elongated porphyroclasts (generally below 13 mm long, but may be considerably larger), and mildly strained to strain-free, rounded to subrounded neoblasts (<0.1 to >1 mm in diameter) along the margin of porphyroclasts, in neoblast domains, and sometimes along kink bands through olivine and orthopyroxene porphyroclasts.

Orthopyroxene in harzburgites is mainly present as large, elongate porphyroclasts (5–6 mm long) with exsolution lamellae of clinopyroxene, rarely spinel, in the cores, and exsolution free rims. Exsolution lamellae are also absent along secondary fluid inclusion trails. A high degree of strain is expressed in undulatory extinction, bent and broken exsolution lamellae (Fig. 3a). The porphyroclasts are invariably surrounded by neoblast aggregates consisting of ol + opx + cpx + sp + silicate glass. Orthopyroxene neoblasts are rare, but are found as rounded to partly rounded, strain-free small grains (<0.2 mm) without exsolution lamella along the boundaries of orthopyroxene porphyroclasts, and as polygonal grains (up to 0.5 mm width) in symplectite (sp + ol + cpx ± opx + silicate glass).

Clinopyroxene typically occurs as small, interstitial grains (<0.1 mm in diameter) in neoblast aggregates, along grain-boundaries of orthopyroxene porphyroclasts, and may, together with silicate glass, fill "cavities" in spongy spinel. Exsolution lamellae or inclusions have not been observed.

Cr-spinel most commonly forms rounded to subrounded grains (0.35–0.5 mm in diameter) with reddish brown cores (in thin-section) and black, spongy rims, sometimes connected into irregular strings (≤3 mm long) along the grain-boundaries of porphyroclasts. These grains are commonly surrounded by narrow domains of glass with microliths of ol + cpx ± opx ± sp. Cr-spinel also occurs as thin, vermicular, grains in a matrix of ol + cpx ± opx + glass ± carbonates (Fig. 3a). These symplectite-like domains usually show embayments into adjacent orthopyroxene and olivine porphyroclasts, and olivine grains in these aggregates may be in optical continu-

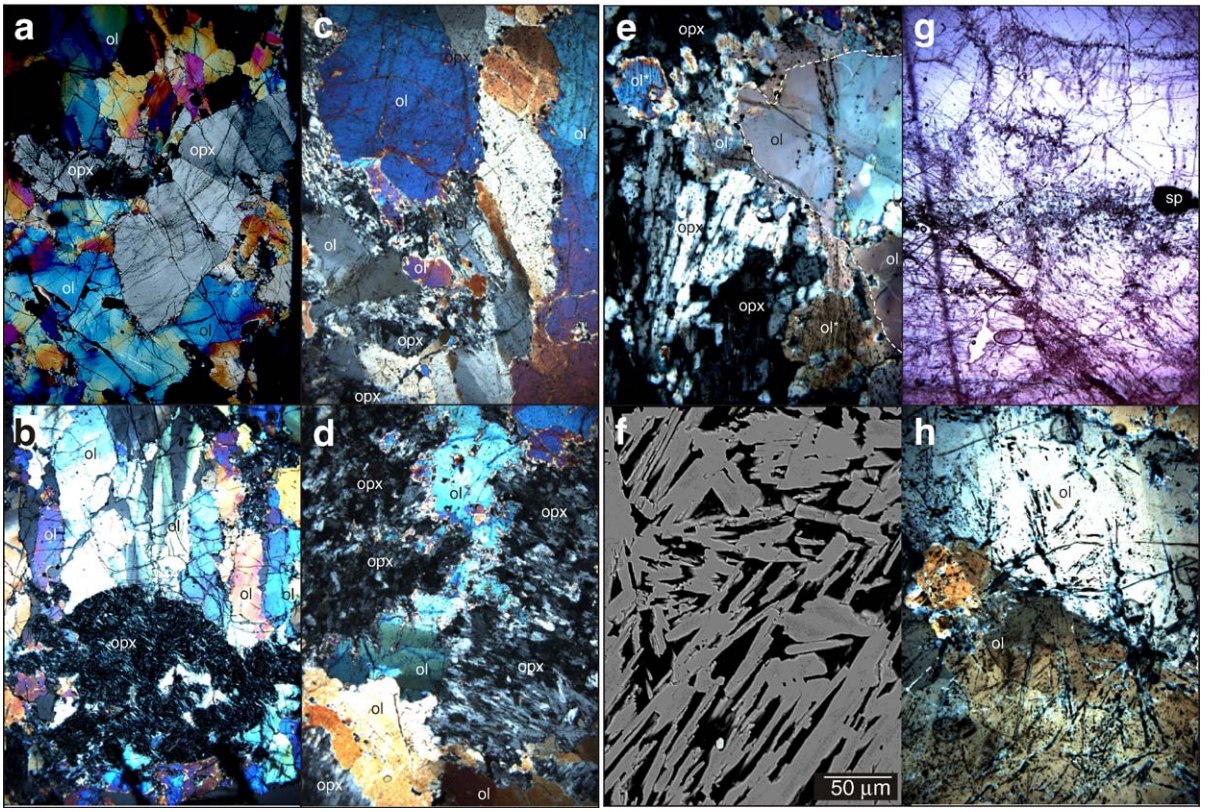

Fig. 3. Photomicrographs showing textural relationships in the mantle xenoliths from Fuerteventura (a) Group A spinel harzburgite (FT9-3) with deformed orthopyroxene and olivine porphyroclasts (ca. 7 × 5 mm, crossed polars). (b) Fibrous orthopyroxene aggregates in Group B spinel harzburgite FBA1-9; the irregular olivine grains inside the fibrous domains are believed to represent remnants after larger grains (ca. 8 × 6 mm, crossed polars). (c) Fibrous orthopyroxene along grain boundaries, partly replacing highly deformed olivine, in Group B spinel harzburgite FBA1-2 (ca. 1.0 × 0.7 mm, crossed polars); (d) remnants of deformed olivine porphyroclasts between domains of fibrous orthopyroxene in Group B spinel harzburgite FBA1-2 (ca. 2.0 × 1.4 mm, crossed polars). (e) Rims of olivine with parallel rows of minute spinel inclusions (ol*) on "clear" olivine porphyroclasts (ol), against domains of fibrous orthopyroxene in Group BC spinel harzburgite TF9-6. The rims are believed to represent growth of olivine at the expense of orthopyroxene with spinel exsolution lamellae. The contact between olivine porphyroclasts and olivine rim (original rim of the olivine porphyroclast) is marked by a white dashed line (ca. 1.0 × 0.7 mm, crossed polars). (f) Scanning microscope image showing domain of fibrous orthopyroxene (pale gray) with numerous cavities (black) and, in the upper left hand area, interstitial glass (medium gray) in Group BC spinel harzburgite FT9-8. (g) Group C spinel dunite FBA1-11 showing deformed olivine porphyroclasts dissected by long, linear polyphase inclusion trails filled by cpx + glass ± sp ± sulfide ± carbonate + fluid (ca. 8 × 6 mm). (h) Close-up of olivine porphyroclasts with linear inclusions trails in sample FBA1-11 (ca. 0.5 × 0.4 mm, crossed polars).

ation with adjacent olivine porphyroclasts, strongly suggesting that these "symplectite" domains formed as the result of reactions involving olivine and orthopyroxene porphyroclasts. Tiny, black euhedral spinel cubes are common in glass pockets, and form randomly scattered inclusions in olivine and pyroxene neoblasts.

Silicate glass (generally transparent) is common interstitially in neoblast domains, and in "symplectites", along cracks and shear planes cutting porphyroclasts, and in fluid inclusions. Interstitial glass commonly contain polygonal, strain-free microphenocrysts (0.3–0.8 mm in diameter) with inclusions of melt ± spinel, scattered randomly throughout the host grain, sometimes concentrated in growth zones; a typical feature of primary inclusions (Roedder, 1984).

Fluid inclusion trails are common, mainly as secondary trails in olivine and orthopyroxene porphyroclasts. They are generally polyphase, consisting of silicate glass + fluid ± silicates ± carbonate. Minute sulfide globules may be present. Orthopyroxene porphyroclasts also contain randomly scattered, isolated inclusions. Networks of vermicular glass + fluid inclusions in the spongy parts of spinel probably represent beginning partial melting, whereas scattered inclusions in the cores of olivine neoblasts are interpreted as primary inclusions trapped during crystal growth. Fluid inclusions are much more common in orthopyr-

oxene than in olivine porphyroclasts, and are less common in olivine in Group A xenoliths than in the other textural groups.

3.2. Group B xenoliths

Group (spinel harzburgites and rare lherzolites) are characterized by the presence of rounded to irregular domains of fibrous orthopyroxene (Fig. 3b). The boundaries between fibrous domains and adjacent olivine may be sharp and regular, or highly irregular. The shapes and sizes of many fibrous domains strongly suggest that they represent pseudomorphs after orthopyroxene phenocrysts, but it is also clear that fibrous orthopyroxene has formed at the expense of olivine (Fig. 3c, d). Disregarding the fibrous domains, the xenoliths in Group B essentially exhibit porphyroclastic to protogranular textures; they are highly deformed, some samples are foliated. The mineral assemblage is the same as in Group A xenoliths, although carbonate and glass pockets are more abundant in the Group B samples. Trace amounts of plagioclase, amphiboles, haüyne$_{SS}$ and rhoenite associated with glass in a few samples are probably the results of reactions/crystallization during ascent, and do not represent mantle processes. The petrographic features that characterize the Group B samples are also seen in Group BC (see below), both Group B and BC samples are therefore used to demonstrate Group B textures in Fig. 3.

Olivine mainly forms large, heavily to mildly kinked porphyroclasts (up to 18 mm long), with bands of olivine neoblast + glass and/or fibrous orthopyroxene along their boundaries and along kink bands. Some porphyroclasts appear as only skeletal remnants between domains of fibrous orthopyroxene (Fig. 3d). Anhedral to subhedral, strain-free olivine neoblasts (<0.1 to >1 mm wide) commonly form clusters along the grain boundaries of, and along kink bands and shear zones inside, olivine porphyroclasts. These neoblast have higher Fo-contents than the coexisting olivine porphyroclasts. Irregular grains of olivine with undulatory extinction may occur within the fibrous aggregates (Fig. 3b, d); such grains may be in optic continuity with olivine porphyroclasts bordering the fibrous domain. Irregular olivine neoblasts inside and adjacent to fibrous orthopyroxene domains commonly have a dusty appearance caused by numerous minute spinel inclusions. Locally these minute inclusions in olivine are oriented in parallel trails (Fig. 3e), suggesting that they represent exsolution lamellae inherited from orthopyroxene which has been replaced by olivine. Small, strain-free, polygonal microliths (<0.4 mm wide) also occur in melt pockets along grain boundaries and in symplectites.

Orthopyroxene mainly forms large, regular to irregular, fibrous domains; each fiber is ≤150 μm long. Such domains may constitute more than 30 vol.% of a sample. The aggregates commonly show embayments against the adjacent olivine grains. In some aggregates the orthopyroxene fibers have random orientations, but most commonly the fibers are oriented along one or two preferred orientations (Fig. 3b–d). In some domains the fibers show sharp kinks where their orientation changes. In these cases we believe the fibers to have inherited their orientation from pre-existing orthopyroxene porphyroclasts. Fibrous domains also form narrow bands inside olivine porphyroclasts (Fig. 3c). The fibrous domains have numerous irregular to rounded cavities, and commonly contain clear glass (Fig. 3f). Locally the fibrous orthopyroxene domains also contain pale brown glass with enclosing subhedral to euhedral strain-free olivine microphenocrysts (0.2–0.6 mm wide) suggesting incipient partial melting. The partial melting that formed these melt zones clearly represent a very late stage; they may have formed during transport of the xenoliths to the surface.

Clinopyroxene is mainly present as small, interstitial, irregular grains in neoblasts domains and along shear plains in olivine porphyroclasts, but also occurs as oriented thin laths in the fibrous orthopyroxene domains, as small, anhedral to subhedral neoblasts in symplectites, and as euhedral microliths in glass. Clinopyroxene typically lacks exsolution lamellae and inclusions.

The mode of occurrence of *Cr-spinel* is essentially as in Group A xenoliths.

Silicate glass most commonly occurs as thin films along grain boundaries (particularly along spinel grains), along fractures in the porphyroclasts, but may also form larger interstitial glass pockets (≤4 mm across) in neoblast domains and in fibrous domains. Microliths of ol ± opx ± cpx ± sp ± carbonate ± fluid are common in the glass. The silicate glass is generally clear and transparent in symplectite, in neoblast areas and in fibrous domains, but may be yellowish brown to brown in melt pockets, in silicate inclusions along shear plans and occasionally in the neoblast domains. Olivine porphyroclasts are commonly traversed by polyphase inclusions trails (± glass ± fluid ± carbonate ± sp) (see description above).

3.3. Group AB xenoliths

Groups AB (spinel harzburgites and rare lherzolites) are transitional between groups A and B, and

contain both orthopyroxene porphyroclasts and fibrous orthopyroxene domains. The fibrous domains commonly occupy the outer parts of orthopyroxene porphyroclasts, and the orthopyroxene fibers are arranged with their long axes along one or two preferred orientations. The fibrous domains appear also to go into olivine porphyroclasts. It seems clear that the fibrous textures are formed partly at the expense of older porphyroclasts.

3.4. Group C xenoliths

Group C (spinel dunites and rare harzburgites) is characterized by the common presence of mottled rims with stringy inclusion trails and spongy rims on large olivine grains. This group lacks orthopyroxene porphyroclasts and large, fibrous orthopyroxene aggregates. Sample FBA1-4 falls in the spinel harzburgite field in Fig. 2, but because of the low proportion of orthopyroxene observed the sample is classified as dunite; the relatively high CaO content (1.2 wt.%) probably results from the numerous silicate glass inclusions. The Group C xenoliths are porphyroclastic and protogranular and consist mainly of ol + sp + cpx. Highly deformed samples show foliation defined by elongated olivine porphyroclasts and subdomains.

Olivine mainly forms strongly deformed porphyroclasts (up to 16 mm long), the margins of, or zones through, which are also commonly dissected by long, linear polyphase trails of inclusions filled by cpx + glass ± sp ± sulfide ± carbonate + fluid; these linear inclusions commonly form a radial pattern (Fig. 3g, h). The rims sometimes appear spongy because of the many inclusion trails. Highly porous domains commonly grade into domains of rounded to sub-rounded olivine neoblasts (<0.07 mm diameter) in a matrix consisting mainly of cpx + sp + glass. Olivine neoblasts occur partly as rounded or subhedral grains (≤0.2 mm across), along kink bands, shear planes, and the margins of olivine porphyroclasts, and partly in symplectite-like domains. Polygonal, strain-free microphenocrysts may be present in interstitial melt pockets. Olivine neoblasts in symplectite domains and olivine microphenocrysts are frequently rich in very small glass ± equant spinel inclusions which may delineate growth zones.

Orthopyroxene has only been observed in sample FBA1-4 as small neoblasts.

Clinopyroxene occurs as small, anhedral to interstitial grains (generally <0.7 mm across) in neoblasts domains, as tiny euhedral crystals (<0.1 mm across) in "symplectite" domains, and as parts of polyphase inclusions.

Cr-spinel forms equant to sub-equant grains (up to 3 mm across) along the margin of olivine porphyroclasts, vermicular grains (up to 1.7 mm long) with ol + cpx + silicate glass in "symplectite-like" domains, and secondary inclusion trails in olivine porphyroclasts and in olivine neoblasts and microphenocrysts. Larger grains are commonly zoned with reddish brown cores and black rims.

Silicate glass (generally transparent) is common along grain boundaries in the neoblasts domain and symplectites, in melt pockets (up to 3 mm across), and along shear planes (yellowish brown to deep brown). Silicate glass is also present, both as glass inclusions, and in polyphase inclusions (glass + -fluid ± sp ± cpx ± carbonate ± sulfide) where fluid is the dominant phase.

3.5. Group BC xenoliths

Group BC xenoliths (spinel harzburgites and rare lherzolites and dunites) show textural features common to both Groups B and C, that is fibrous orthopyroxene aggregates as well as olivine porphyroclasts with spongy rims and lots of stringy inclusion trails. Fibrous and fine-grained domains of orthopyroxene commonly form networks criss-crossing olivine porphyroclasts. Below we refer to these textures together as "fibrous textures". Whereas as the cores of olivine porphyroclasts are clear outside fluid inclusion trails, olivine in, or adjacent to, fine-grained areas commonly have a dusty appearance due to large amounts of minute spinel inclusions. Like in Group B xenoliths these minute spinel inclusions may form parallel trails. In some samples (e.g. FT 9-8 and FT 9-10) fibrous orthopyroxene aggregates contain large, irregular spinel grains (up to 12 mm across) which may enclose clusters of fibrous orthopyroxene.

3.6. Group D xenoliths

Some spinel harzburgites and lherzolites are predominantly fined-grained and equigranular, with a mean grain size <1 mm, without foliation or layering. FT9-1 consists mainly of olivine (up to 0.6 mm across) in a finer-grained matrix composed mainly of ol + opx + cpx + sp; glass is common in the matrix. Highly irregular, highly deformed olivine grains (<2 mm wide) are common. These grains, which are commonly cloudy due to trails of tiny secondary inclusions, are interpreted as remnants of an earlier generation of larger, strongly deformed grains. Spinel may form sub-rounded (1 mm across), holly-leaf shaped (6 mm

long), dust-like grains scattered inside and along the margins of silicate grains, and vermicular grains (2 mm long) in symplectite-like domains. Large Cr-spinel grains commonly have broad red brown cores and thin black rims. Sample FBA1-23 (lherzolite) is very fine-grained and contains significant proportions of interstitial, light brown glass.

3.7. Spinel wehrlite

The spinel wehrlite (sample FT9-15) is mildly deformed, coarse-grained and equigranular. Olivine forms equidimensional, mildly strained grains (diameter ≤4 mm). Clinopyroxene (≤1.6 mm) is generally present as poikilitic, interstitial grains that enclose olivine, orthopyroxene and spinel, whereas Cr-spinel mainly forms subhedral to irregular, interstitial grains (0.7 mm), but is also found as tiny inclusions in olivine and clinopyroxene grains. Domains of smaller neoblasts of olivine, clinopyroxene, glass and Cr-spinel occur locally along grain boundaries and in triple junctions. Trace amounts of small orthopyroxene tablets and plagioclase are also present. Exsolution lamellae in clinopyroxene have not been observed. Silicate glass is present interstitially, as thin rims around some Cr-spinel grains, as primary inclusions in the neoblast and spinel grains, and as secondary inclusion trails in the olivine grain.

4. Analytical methods

Minerals and glasses were analyzed for major elements using a CAMECA CAMEBAX S×100 electron microprobe at department of Geology, the University of Oslo. Accelerating voltage was 15 kV and peaks were counted for 10 s and backgrounds for 5 s using a beam current of 20 nA and focused beam. Light elements were counted first to preclude loss by volatilization. Oxides, natural and synthetic standards have been used. Matrix corrections were performed by the PAP-procedure in the CAMECA software. Analytical precision (±2 sigma error) evaluated by repeated analyses of individual grains is better than ±1% for elements in concentrations of >20 wt.% oxide, better than ±2% for elements in the range 10–20 wt.% oxide, better than 5% for elements in the range 2–10 wt.% oxide, and better than 170% for elements in the range 0.5–2 wt.% oxide.

Major elements in bulk rocks were determined by X-ray fluorescence spectrometry (XRF) at the Department of Earth Sciences, University of Bergen, using glass fusion discs and pressed powder tablets and international standards for calibration.

Table 1
Representative olivine analyses (wt.%)

Group	Group A					Group B			Group AB				Group C		Group BC		Group D	Wehrlite
Sample	FBA1-8	FT9-27	FT9-4		FT9-12	FBA1-7		FBA1-1	FT9-5				FBA1-4		FT9-7		FT9-1	FT9-15
Rock type	Lherz	Harz	Dunite		Dunite	Lherz		Dunite	Harz				Dunite		Harz		Harz	Wehrlite
Description	Porph core	Porph core	Porph core	Rim	Porph	Neoblast sheared	Porph core	Sympl	Porph core	Sympl	Neobl	Ass fibr opx	Porph core	Spongy rim	Porph	Ass fibr opx	Neoblast small	Large core
SiO_2	41.31	40.88	39.25	39.25	40.84	41.37	40.77	39.89	40.42	39.69	40.18	40.55	41.08	41.55	41.35	41.91	39.98	40.35
FeO	8.81	8.63	16.89	18.19	8.01	6.56	8.43	12.78	7.85	10.52	11.42	8.77	7.84	7.34	8.35	7.01	11.89	10.38
MnO	0.11	0.12	0.23	0.29	0.13	0.15	0.13	0.22	0.14	0.12	0.20	0.12	0.13	0.14	0.13	0.09	0.19	0.19
MgO	49.61	49.99	43.41	41.72	50.19	51.46	50.05	46.48	50.37	47.92	48.03	50.00	50.86	51.18	49.63	50.55	47.50	48.41
CaO	0.04	0.05	0.12	0.36	0.13	0.05	0.10	0.31	0.09	0.16	0.22	0.14	0.03	0.12	0.04	0.11	0.17	0.12
NiO	0.39	0.37	0.22	0.31	0.39	0.30	0.32	0.25	0.36	0.36	0.26	0.42	0.37	0.38	0.42	0.35	0.21	0.30
Total	100.26	100.04	100.13	100.25	99.68	99.96	99.79	99.93	99.22	99.50	100.07	100.30	100.00	100.70	99.92	100.01	99.94	99.74
Fo	90.9	91.2	82.1	80.4	91.8	93.3	91.4	86.6	92.0	91.2	92.1	91.2	87.9	91.0	92.0	92.6	91.4	92.8	87.7	89.3

Porph: porphyroclast; spongy r: spongy rim; ass fibr opx: irregular grain in domain of fibrous orthopyroxene; microph: microphenocrysts associated with silicate glass; sympl: symplectite; Fo: forsterite content. The textural characteristics of the different groups are explained in the text.

Table 2
Representative orthopyroxene analyses (wt.%)

Group	Group A						Group B		Group AB			Group C	Group BC			Group D
Sample	FT9-9	FT9-27			FT9-12	FT9-14	FBA1-1	FBA1-7	FT9-5			FBA1-4	FBA1-3	FT9-2	FT9-7	FT9-1
Rock type	Harz	Harz			Dunite	Dunite	Dunite	Lherz	Harz			Harz	Harz	Harz	Harz	
Description	Porph core	Porph core	Neoblast		Neoblast ass sp	Neoblast	Fibrous ass sp	Fibrous	Porph		Fibrous	Neoblast	Fibrous	Fibrous	Fibrous	Medium
			core	rim					core	spongy r						
SiO_2	57.04	55.65	56.69	56.10	53.76	59.00	56.92	56.67	57.34	57.95	56.71	58.12	56.35	58.16	57.91	55.72
TiO_2	0.02	0.02	0.02	0.01	0.01	0.04	0.01	0.07	0.01	0.07	0.05	0.10	0.29	0.01	0.02	0.03
Al_2O_3	1.75	2.08	1.27	1.65	5.68	0.25	0.70	0.52	2.03	1.13	1.06	0.70	1.19	0.59	1.55	1.37
Cr_2O_3	0.51	0.78	0.97	1.44	0.34	0.01	0.31	0.44	0.79	0.63	0.48	0.19	0.48	0.03	0.64	0.44
FeO	5.49	5.49	5.76	6.12	7.02	4.91	4.76	5.11	5.48	4.96	5.25	5.00	5.01	4.46	3.88	6.89
MnO	0.15	0.13	0.17	0.16	0.13	0.17	0.11	0.13	0.13	0.11	0.12	0.12	0.09	0.11	0.06	0.14
MgO	33.82	33.63	34.79	33.80	32.39	35.50	35.41	34.41	34.00	34.76	34.87	35.08	34.67	36.43	35.36	33.63
NiO	0.06	0.09	0.09	0.03	0.11	0.16	0.14	0.11	0.10	0.10	0.11	0.13	0.13	0.21	0.12	0.09
CaO	0.93	1.41	0.82	1.57	0.13	0.94	1.05	1.66	1.47	1.28	1.25	0.91	1.43	0.61	0.74	1.08
Na_2O	0.02	0.04	0.12	0.01	0.02	0.06	0.07	0.09	0.03	0.03	0.04	0.02	0.01	0.02	0.03	0.04
Total	99.83	99.32	100.70	100.89	99.54	101.06	99.50	99.22	101.38	101.01	99.94	100.38	99.63	100.64	100.33	99.42
mg#	91.7	91.6	91.5	90.8	89.1	92.8	93.0	92.3	91.7	92.6	92.2	92.6	92.5	93.6	94.2	89.7

Harz: harzburgites; lherz: lherzolite; porph: porphyroclast; spongy r: spongy rim; neobl: neoblast; ass sp: small grain associated with spinel, commonly also silicate glass; sympl: symplectite; mg#: cation proportion Mg*100/(Mg+Fe). The textural characteristics of the different groups are explained in the text.

Table 3
Representative clinopyroxene analyses (wt.%)

Group	Group A											Group B			Group BC					Group D		Wehrlite	
Sample	FBA1-8			FT9-3		FT9-9		FBA1-12	FT9-28			FBA1-1			FT9-2		FT9-8			FT9-1		FT9-15	
Rock type	Lherz			Harz		Harz		Dunite	Dunite			Dunite			Harz		Harz			Harz		Wehrlite	
	Neoblast	Microphen ass sp	Microphen ass sp	Neoblast	Neoblast	Neobl	Microphen	Neoblast	Neoblast	Incl in ol	Neoblast ass sp	Incl in ol	Ass fibr opx	Neoblast	Neoblast	Neoblast	Neoblast	Neoblast	Ass fibr opx	Medium core	Rim	Neoblast	Neoblast
SiO_2	54.62	52.83	52.28	54.74	53.95	54.52	54.27	51.10	50.07	51.83	44.84	52.96	54.35	53.28	54.59	54.41	52.81	49.51	55.67	51.78	51.92	53.77	52.24
TiO_2	0.03	0.01	0.08	0.01	n.d.	0.03	0.03	0.22	1.56	1.01	4.21	0.18	n.d.	0.63	0.56	0.16	n.d.	0.01	0.01	0.85	0.97	0.29	0.38
Al_2O_3	1.28	2.65	5.03	1.02	1.75	1.41	1.02	4.69	4.04	3.35	8.90	3.30	1.24	1.19	1.06	1.31	2.62	5.49	1.65	2.98	2.84	1.47	3.27
Cr_2O_3	0.44	1.31	1.97	0.84	0.76	0.66	1.05	0.85	1.38	0.21	1.13	0.91	0.38	0.97	0.33	0.88	0.20	0.70	0.44	1.04	0.74	0.92	1.06
FeO	1.55	3.28	3.30	2.74	2.31	2.26	3.09	3.92	2.77	2.63	3.86	3.97	3.37	3.20	2.96	3.59	3.10	3.71	1.30	4.77	4.83	2.77	3.16
MnO	0.05	0.17	0.16	0.10	0.07	0.07	0.02	0.35	0.05	0.10	0.03	0.03	0.13	0.09	0.11	0.10	0.33	0.32	0.29	0.16	0.11	0.10	0.02
MgO	18.71	17.33	17.32	19.11	17.85	18.49	19.72	15.41	15.66	17.01	12.98	17.10	20.38	18.75	19.64	19.02	17.48	15.21	19.01	16.94	17.17	17.93	15.89
NiO	0.38	0.32	0.28	0.05	0.05	0.12	0.13	0.05	0.07	0.06	0.11	0.01	0.08	0.04	0.11	0.08	0.03	0.06	0.08	0.02	0.08	0.05	0.04
CaO	23.44	20.75	20.29	21.36	23.42	22.43	20.33	23.31	23.74	23.82	23.48	19.27	19.38	20.02	20.70	20.68	23.39	24.34	20.47	21.32	20.99	22.17	23.48
Na_2O	0.20	0.34	0.41	0.27	0.12	0.27	0.33	0.54	0.39	0.29	0.45	0.67	0.25	0.82	0.37	0.49	0.13	0.06	0.64	0.49	0.51	0.55	0.55
Total	101.14	99.37	101.51	100.59	100.70	100.68	100.30	100.45	99.71	100.30	99.98	98.53	99.56	98.98	100.45	100.72	100.08	99.41	99.54	100.36	100.18	100.04	100.10
mg#	95.6	90.4	90.3	92.6	93.2	93.6	91.9	87.5	91.0	92.0	85.7	88.5	91.5	91.2	92.2	90.4	90.9	88.0	96.3	86.4	86.4	92.0	90.0

Porph: porphyroclast; spongy r: spongy rim; neobl: neoblast; ass sp: small grain associated with spinel, commonly also silicate glass; ass fibr opx: interstitial grain in domain of fibrous orthopyroxene; microph: microphenocrysts associated with silicate glass; sympl: symplectite; n.d.: not detected; mg#: cation proportion Mg*100/(Mg+Fe). The textural characteristics of the different groups are explained in the text.

Table 4
Representative spinel analyses (wt.%)

Group	Group A								Group B			Group AB			Group C		Group BC		Group D		Wehrlite			
Sample	FBA1-8		FT9-3	FT9-32	FT9-4	FT9-13	FT9-28		FBA1-1		FT9-21	FT9-5			FBA1-4		FT9-2		FT9-1		FT9-15			
Rock type	Lherzolite		Harz	Harz	Dunite	Dunite	Dunite		Dunite		Dunite	Harzburgite			Dunite		Harzburgite		Harzburgite		Wehrlite			
	Large		Symplectite	Symplectite	Large spongy	Large spongy	Medium		Symplectite		Large spongy	Large spongy		Microphen	Symplectite		Occurrence granular		Large massiv		Large spongy		Large spongy	
	massiv c	spongy r	spongy c	spongy c	core	core	massiv c	massiv r	core	rim	core	core	rim		core	rim	core	rim	core	rim	core	rim	core	rim
TiO2	0.03	0.01	0.09	0.29	2.09	0.62	0.44	2.02	0.08	0.08	0.29	0.02	1.54	3.45	0.02	2.32	n.d.	3.82	0.01	2.26	1.04	1.87	1.62	1.14
Al_2O_3	25.31	19.84	16.26	11.43	12.98	31.41	25.58	11.93	2.82	5.19	30.21	20.87	12.78	10.86	19.59	5.04	22.84	13.06	23.80	10.41	7.10	8.67	14.29	18.81
Cr_2O_3	44.86	49.13	52.60	58.76	31.21	33.01	41.12	37.63	36.88	36.46	36.67	48.15	49.85	46.86	46.79	31.97	46.14	38.49	42.87	36.68	31.11	30.68	36.12	34.12
Fe_2O_3	0.48	1.32	1.58	0.93	11.18	3.04	1.88	9.58	16.14	15.12	1.73	1.52	3.18	3.24	3.14	16.08	1.22	6.69	1.78	10.03	15.80	14.44	9.21	8.46
FeO	14.86	15.63	14.76	15.03	31.92	13.79	15.52	24.60	32.59	31.61	13.45	15.23	20.40	24.85	14.76	30.00	15.40	24.59	17.80	28.63	32.62	32.45	24.50	20.57
MnO	0.21	0.14	0.27	0.24	0.23	0.16	0.26	0.21	0.18	0.22	0.16	0.18	0.28	0.33	0.21	0.23	0.24	0.27	0.25	0.28	0.18	0.17	0.21	0.25
MgO	13.93	13.30	13.58	12.74	8.61	16.94	14.41	12.34	8.70	8.98	15.99	13.85	11.36	9.23	14.89	11.91	13.67	11.92	12.40	9.94	9.52	9.61	12.16	14.34
NiO	0.06	0.10	0.10	0.03	0.29	0.19	0.18	0.26	0.35	0.42	0.14	0.15	0.12	0.19	0.09	0.33	0.10	0.23	0.09	0.17	0.24	0.22	0.25	0.29
Total	99.75	99.46	99.41	99.46	97.50	98.99	99.25	97.71	97.73	98.07	98.63	99.96	99.51	99.02	99.48	97.89	99.60	99.07	98.99	98.41	97.62	98.10	98.37	97.96

C: core; r: rim; microphen: microphenocrysts in glass; incl ol: inclusion in ol; n.d.: not detected. Fe_2O_3 is estimated on the basis of 3 cations and 4 oxygens in the structural formula. The textural characteristics of the different groups are explained in the text.

Table 5
Representative whole rock major element compositions (wt.%)

Group	Group A							Group B			Group AB		Group C			Group BC				Group D		Wehrlite
Sample	FBA1-8	FT9-9	FT9-32	FBA1-12	FBA 1-16	FBA1-19	FT9-4	FBA1-2	FBA1-7	FBA1-22	FA1-1	FT9-33A	FT9-5	FBA 1-4	FBA1-11	FBA1-15	FT9-6	FT9-10	FBA1-13	FT9-1	FBA1-23	FT9-15
Rock type	Lherz	Harz	Harz	Dun	Dun	Dun	Dun	Harz	Lherz	Harz	Dun	Lherz	Harz	Dun	Dun	Lherz	Harz	Harz	Dun	Harz	Lherz	Wehrlite
SiO_2	40.78	43.79	42.42	39.41	39.10	39.49	38.53	42.56	41.74	41.98	38.80	40.84	42.63	41.57	40.04	40.66	42.38	42.53	39.89	43.06	40.53	40.05
TiO_2	0.10	0.02	0.03	0.03	0.12	0.03	0.02	0.06	0.29	0.07	0.02	0.09	0.06	0.19	0.07	0.20	0.06	0.17	0.05	0.14	0.91	0.13
Al_2O_3	1.13	0.42	0.51	0.34	0.74	0.51	0.08	0.44	1.24	0.38	0.40	3.67	0.46	0.91	0.24	0.76	0.32	0.80	0.61	1.20	4.18	1.10
FeO_{total}	10.70	7.69	8.58	10.50	10.89	8.73	16.99	7.74	9.21	8.13	10.03	9.39	8.05	8.05	8.13	9.23	7.98	8.34	9.42	7.89	9.37	10.51
MnO	0.16	0.12	0.14	0.16	0.19	0.14	0.26	0.14	0.16	0.14	0.15	0.15	0.12	0.14	0.14	0.16	0.12	0.13	0.15	0.16	0.20	0.17
MgO	44.21	46.34	46.17	48.57	47.33	50.08	42.85	47.94	44.39	48.06	49.18	39.71	46.02	46.12	50.39	45.84	47.34	44.78	49.02	43.85	37.60	44.14
CaO	2.91	0.49	0.76	0.47	0.80	0.49	0.31	0.72	2.36	1.11	0.24	3.51	0.72	1.21	0.50	2.22	0.66	1.38	0.73	1.10	3.49	1.78
Na_2O	0.11	0.09	0.11	0.10	n.d.	0.10	0.11	0.07	0.06	0.07	0.10	0.13	0.09	0.03	n.d.	0.07	0.07	0.06	0.11	0.05	0.15	0.08
K_2O	n.d.	0.01	n.d.	n.d.	0.01	n.d.	n.d.	n.d.	0.02	0.01	n.d.	0.01	0.01	0.02	n.d.	0.01	n.d.	0.03	n.d.	0.04	0.18	0.01
P_2O_5	0.01	0.01	n.d.	0.01	n.d.	n.d.	0.01	n.d.	n.d.	n.d.	0.01	0.02	0.01	n.d.	n.d.	n.d.	n.d.	0.01	0.01	0.01	0.14	0.01
LOI	n.d.	n.d.	n.d.	n.d.	n.d.	n.d.	n.d.	n.d.	n.d.	n.d.	n.d.	n.d.	n.d.	n.d.	n.d.	0.21	n.d.	n.d.	n.d.	n.d.	0.23	n.d.
SUM	100.11	98.98	98.72	99.59	99.18	99.57	99.16	99.67	99.47	99.95	98.93	97.52	98.17	98.24	99.51	99.36	98.93	98.23	99.99	97.50	96.98	97.98
mg#	88.0	91.5	90.6	89.2	88.6	91.1	81.8	91.7	89.6	91.3	89.7	88.3	91.1	91.1	91.7	89.8	91.4	90.5	90.3	90.8	87.7	88.2

Harz: harzburgites; lherz: lherzolite; dun: dunite; wehr: wehrlite; LOI: loss on ignition; n.d.: not detected; mg#: cation proportion Mg*100/(Mg+Fe). The textural characteristics of the different groups are explained in the text.

Representative mineral and whole rock analyses are given in Tables 1–5, and in Electronic Appendix table which may be downloaded from the *Lithos* web site at http://www1.elsevier.com/pub/9/17/elan.htt?jnl=lithos.

5. Mineral chemistry

5.1. Spinel harzburgites and lherzolites

The olivine in the spinel harzburgite and lherzolite xenolith from Fuerteventura covers a wide range in compositions. However, most cores of porphyroclasts (including all Group A samples) fall within the restricted range $Fo_{90.7–91.4}$, 0.36–0.41 wt.% NiO, and CaO < 0.10 wt.%, that is within, and close to, the field of Mid-Atlantic Ridge mantle south of the Kane Fracture Zone (MARK: the MARK area is that part of the Atlantic Ridge for which data are available that lies closest to the Canary Islands; Table 1; Fig. 4a, b). The low CaO contents in the porphyroclasts are typical of olivine in mantle rocks (Yaxley et al., 1998). The olivine neoblasts and rims of porphyroclasts cover wider compositional ranges (Fig. 4). The lowest Fo-contents are found in neoblasts in Groups AB, BC and D, whereas olivine associated with fibrous orthopyroxene in Group BC shows the highest Fo-contents. The highest CaO contents (up to 0.25 wt.%) are found in the most Fe-rich olivine. The microphenocrysts show an even wider range in Fo-contents than the neoblasts ($Fo_{86.6–94.0}$), and show similar CaO–Fo relationships as the neoblasts (0.08–0.32 wt.% CaO), but tend towards lower NiO contents.

Also the cores in orthopyroxene porphyroclasts (Groups A and AB) show a very restricted compositional range (e.g. mg# = cation proportion $Mg*100/(Mg+Fe_{total})$ = 91.3–91.7, ≤0.02 wt.% TiO_2, 1.5–2.2 wt.% Al_2O_3; Table 2; Fig. 5) that lies within, or close to, the most Ti–Al–Ca depleted part of the MARK field.

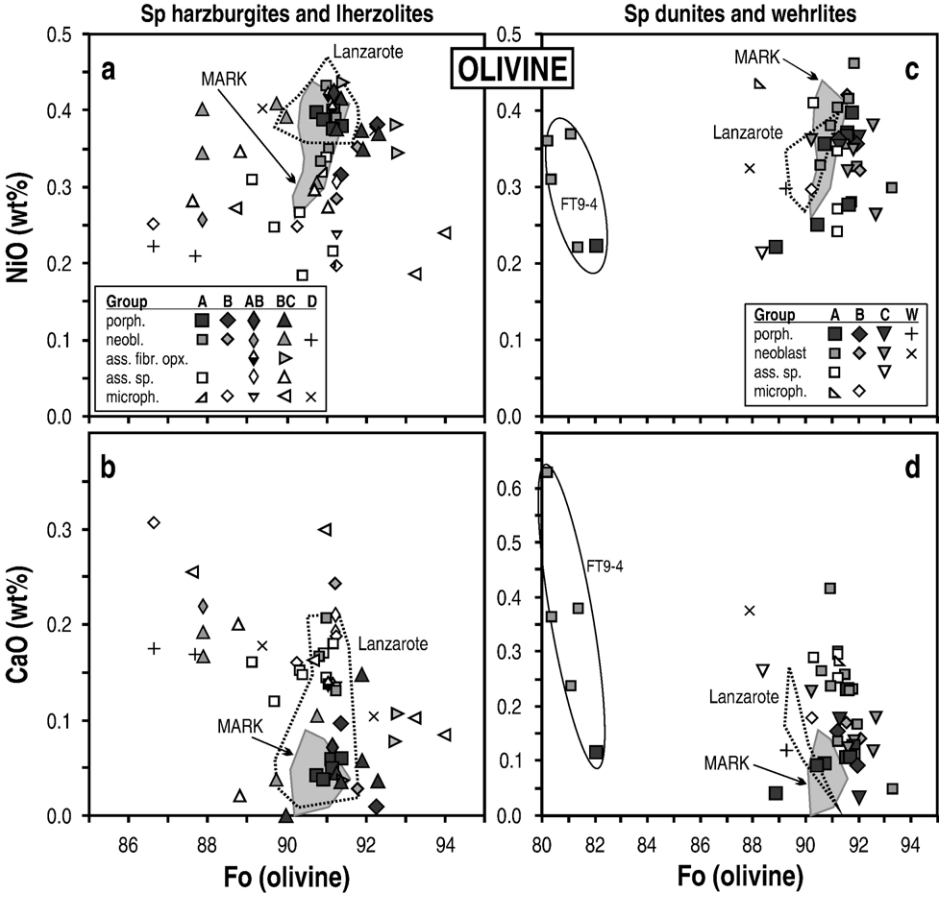

Fig. 4. Concentrations of NiO and CaO plotted against forsterite content (Fo) in olivine in mantle xenoliths from Fuerteventura, compared to peridotite xenoliths collected along the mid-Atlantic Ridge, south of the Kane Fracture Zone about 23° N (*MARK*: Komor et al., 1990; Niida, 1997; Ross and Elthon, 1997; Stephens, 1997). The MARK area is that part of the Atlantic Ridge for which data are available that lies closest to the Canary Island.

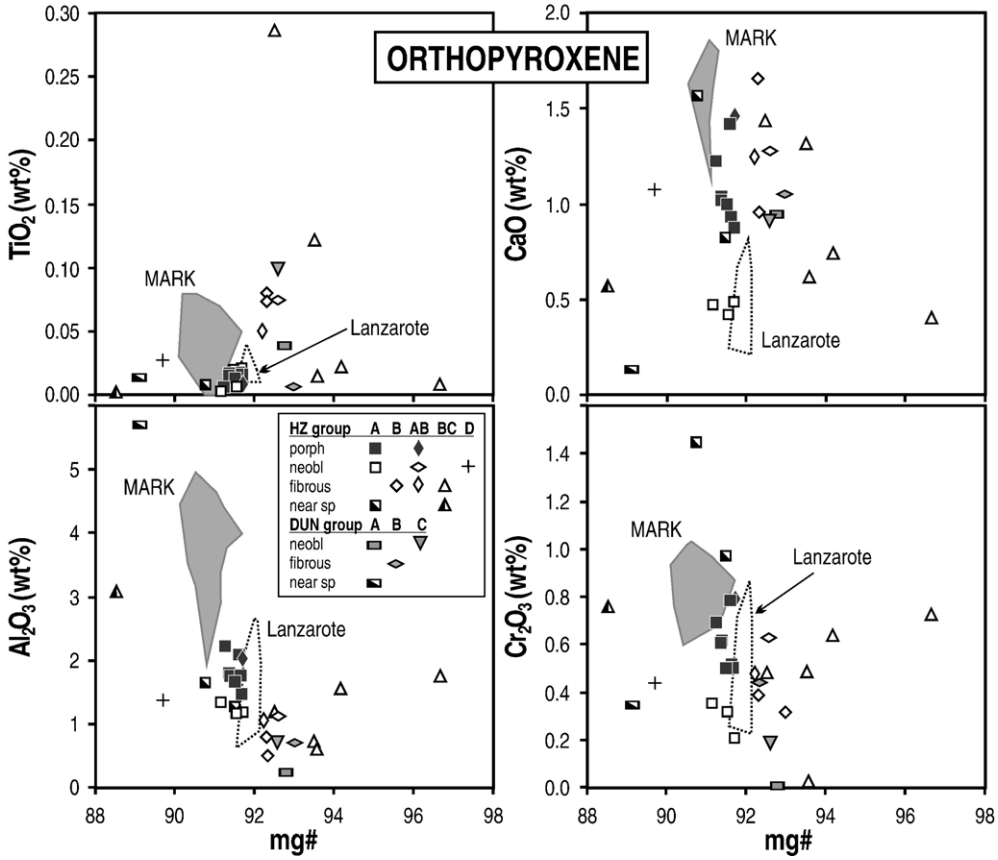

Fig. 5. Chemical variations among orthopyroxene in mantle xenoliths from Fuerteventura. For comparison we also show orthopyroxene in mantle rocks collected in the MARK area (references given for Fig. 4). *MARK*: See the caption of Fig. 4. *Dun*: dunite; *porph*: cores in porphyroclasts; *neoblasts*: rims on porphyroclasts and granular neoblasts; *fibrous*: fibrous orthopyroxene; *near sp*: orthopyroxene associated with spinel.

The porphyroclasts commonly show zoning with increasing Al_2O_3, Cr_2O_3 and CaO from core to rim, but in sample FT9-5, Al_2O_3 and Cr_2O_3 decrease and mg# increases from core to rim (Table 2; Fig. 5). Rims on orthopyroxene porphyroclasts, neoblasts in symplectites and in other neoblast domains tend towards higher mg# (91.2–92.6) and TiO_2, and lower concentrations in Al_2O_3, CaO and Cr_2O_3 (Table 2, Fig. 5) than the porphyroclast cores, whereas orthopyroxene in Group D and grains associated with spinel are less magnesian. All analyzed fibrous orthopyroxene are more magnesian than the porphyroclast cores (mg#: 92.2–97.0; Table 2, Fig. 5), and they show a rough trend of decreasing TiO_2 and CaO with increasing mg#.

Clinopyroxene shows a wide compositional range both within and between samples, and the composition of individual grains appears to some degree to be related to the neighboring phase assemblages. In general the clinopyroxenes have lower concentration in Al_2O_3 and Cr_2O_3, and higher contents of TiO_2 and Na_2O than clinopyroxenes in peridotites in the MARK area (Table 3; Fig. 6a–d). Clinopyroxene neoblasts associated with olivine and orthopyroxene in Group A cover a restricted compositional range compared to those in Groups B, AB and BC. The highest mg# is found in clinopyroxene associated with fibrous orthopyroxene in Group BC, whereas clinopyroxene in Group D, clinopyroxene associated with Cr-spinel, and clinopyroxene microphenocrysts tend towards lower mg# (86.4–92.2), and higher concentrations in TiO_2 (<0.01–2.5 wt.%) and Al_2O_3 (0.7–5.0 wt.%) than clinopyroxene associated with olivine and orthopyroxene porphyroclasts (Fig. 6).

Cr-spinel shows significant compositional differences, both between the different petrographic groups, and on the scale of a thin-section. In Group A the cores of large spinel grains are enriched in Cr relative to Al and have very low contents of Ti (≤0.002 cations) and Fe^{3+} (≤0.032 cations, based on 3.000 cations and 4.000 oxygens in the structural formulae; Table 4, Fig. 7a–c). The Ti and Fe^{3+} contents in Group A spinels are within the range of spinel in oceanic peridotites, but they are more enriched in Cr relative to Al. Spinel in

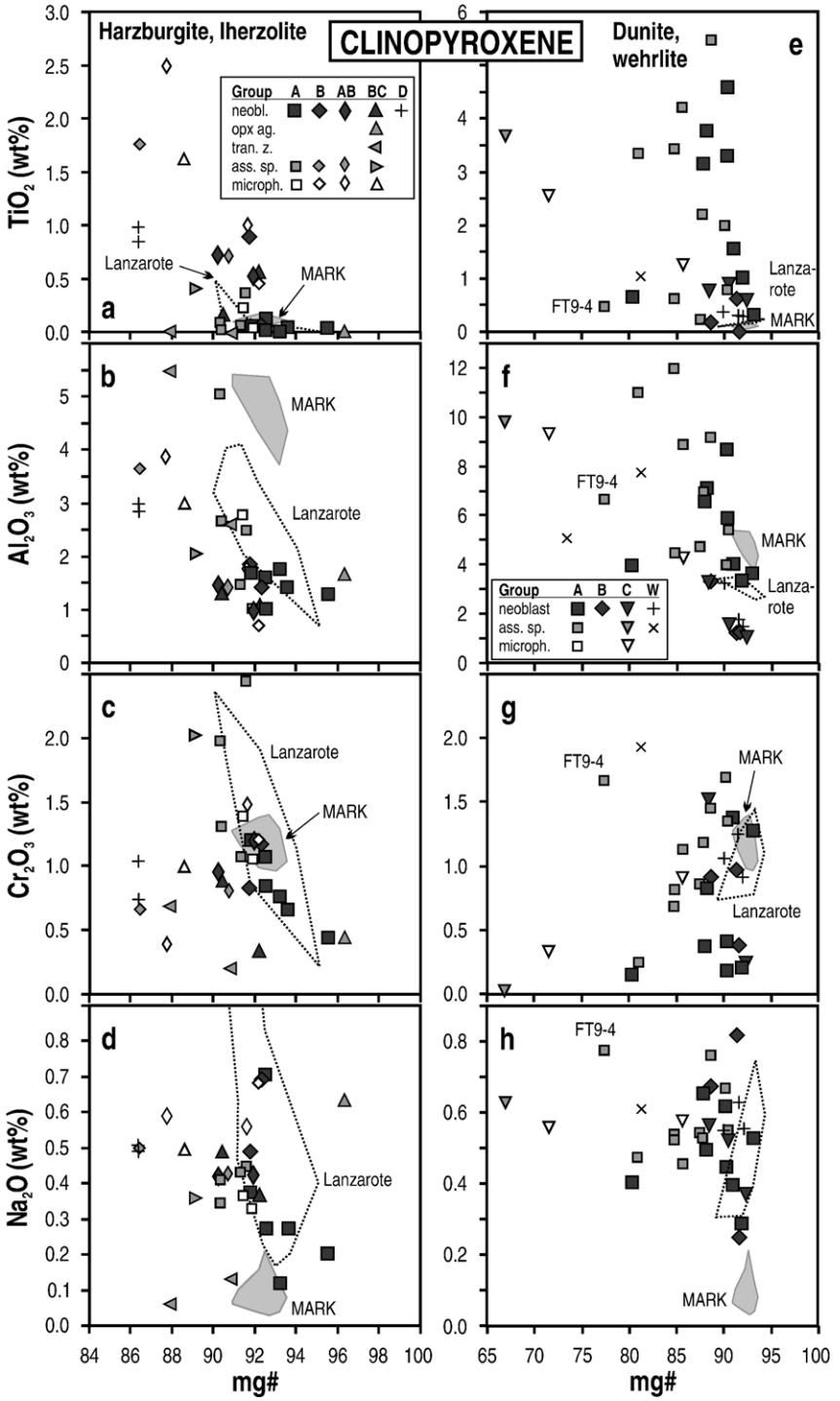

Fig. 6. Chemical variations among clinopyroxene in mantle xenoliths from Fuerteventura. For comparison are also shown the compositional ranges of clinopyroxene in mantle rocks collected in the MARK area (Niida, 1997; Ross and Elthon, 1997; Stephens, 1997).

symplectites in Group A are slightly more Cr-rich but has low Ti and Fe^{3+} contents. Compositional variations on the scale of a thin-section is usually interpreted as evidence of local disequilibria (e.g., Henry and Medaris, 1980; Sen and Presnall, 1986). There is a clear tendency for increasing Ti and Fe^{3+}, and decreasing mg# from Group A through Groups AB to Groups B, BC and D (Fig. 7).

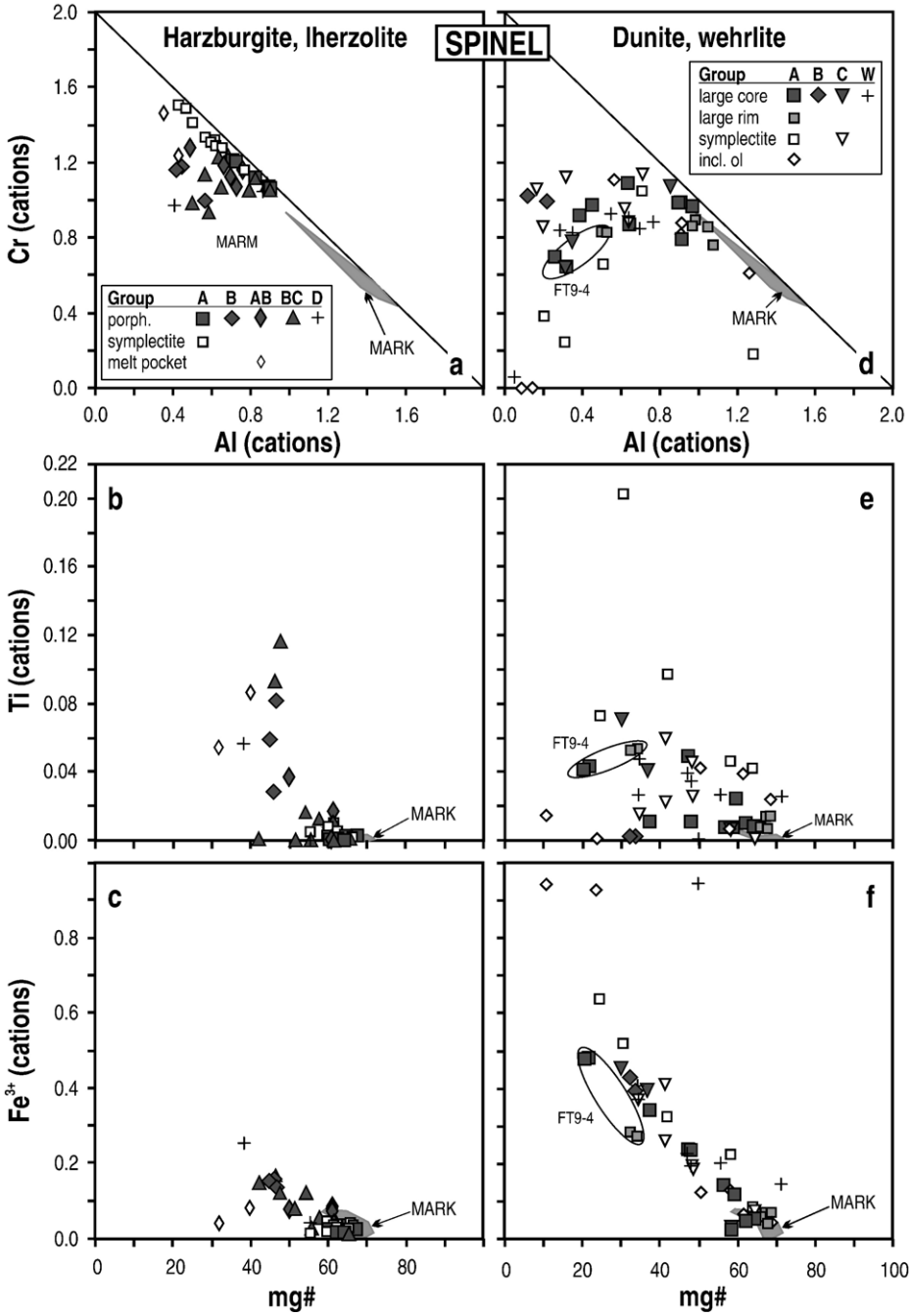

Fig. 7. Chemical variations among spinel in mantle xenoliths from Fuerteventura. For comparison are also shown the compositional ranges of spinel in mantle rocks collected in the MARK area (Niida, 1997; Ross and Elthon, 1997; Stephens, 1997). *MARK*: See the caption of Fig. 4.

5.2. Spinel dunites and wehrlites

With the exception of sample FT9-4, olivine in dunites and wehrlites covers the ranges $Fo_{87.9–93.3}$, and has up to 0.31 wt.% CaO (Table 1; Fig. 4). In the Fe-rich sample FT9-4, the olivine composition is about Fo_{81}.

Orthopyroxene neoblasts in the dunites are slightly more magnesian than the neoblasts in the harzburgite samples (mg#=92.6–93.0), and they have higher TiO_2 and lower Al_2O_3 contents (Table 2; Fig. 5).

Clinopyroxene in the dunites and wehrlites are less magnesian (mg#=67–93; Table 3; Fig. 6e–h), are in general significantly richer in TiO_2 (0.2–5.5 wt.%) and

Al_2O_3 (1.1–12.0 wt.%) than clinopyroxene in the harzburgites. Most granular neoblasts fall in the high-mg# part of the mg#-range, whereas clinopyroxene associated with spinel are less Mg-rich.

As compared to harzburgites and lherzolites, spinel in dunites and wehrlites are, on the average, richer in Ti, and are significantly richer in Fe^{3+} and Fe^{2+} (Table 4; Fig. 7c–f), although some spinels in Group A-dunites fall within the range of porphyroclast cores in Group A harzburgites. The highest Ti, Fe^{3+} and Fe^{2+} contents are found in spinel in symplectites and inclusions in olivine in Group A, as well as in the Fe-rich Group A sample FT9-4 (Table 4; Fig. 7). Spinel in the dunites shows a clear trend of increasing Fe^{3+} with decreasing mg#.

6. Whole rock chemistry

Seen together, the mantle xenoliths from Fuerteventura show considerable compositional variety (e.g. mg#=81.8–91.8; Table 5; Fig. 8). The harzburgites in Group A, however, fall within a relatively restricted range which for most major elements partly overlap the field of Mid-Atlantic Ridge (MAR) peridotites (e.g. mg#=90.6–91.5; Fig. 8). As a group, the Group A harzburgites has the lowest TiO_2, Al_2O_3, and CaO, and the highest Na_2O contents among the Fuerteventura peridotites. The harzburgites in the other groups cover the same range in mg# as those in Group A, but are richer in TiO_2, Al_2O_3 and CaO, and more depleted in Na_2O (Fig. 8). The lherzolites have lower SiO_2 and mg# and higher CaO contents than the harzburgites, and their compositions include the highest TiO_2 and Al_2O_3 concentrations. The lowest mg# (87.7) and highest TiO_2, Al_2O_3 and CaO concentrations among the harzburgites/lherzolites are found in the fine-grained Group D sample FBA1-23 (Fig. 8). Together, the harzburgites and lherzolites define rough trends of decreasing SiO_2 and MgO, and increasing TiO_2, Al_2O_3, CaO and Na_2O with decreasing mg#, which roughly overlap with the trend from depleted harzburgites to strongly metasomatized harzburgites and lherzolites defined by mantle rocks from Tenerife (Neumann et al., 2002; Fig. 8). With one exception the dunites fall within the mg# range 88.6–91.8, the exception is sample FT9-4 with mg#=81.8 (not shown in Fig. 8). The low mg# of this sample is clearly not a primary feature. The high-mg# dunites have lower SiO_2 and higher MgO contents than the harzburgites and lherzolites, but fall within the same ranges with respect to TiO_2, Al_2O_3 and Na_2O (Fig. 8).

7. Discussion

The textural relationships in the mantle xenoliths from Fuerteventura imply that the oldest petrographic features are represented by the olivine and orthopyroxene porphyroclasts in the Group A (and AB) harzburgites. The "fibrous textures" (fibrous orthopyroxene aggregates, spongy rims and lots of long, radial inclusions in olivine porphyroclasts, fibrous and fine-grained domains of orthopyroxene criss-crossing olivine porphyroclasts) which characterize Group AB, B, C and BC xenoliths clearly overprint, and are younger than, the porphyroclasts. Also the neoblasts appear to a large extent to have formed at the expense of porphyroclasts and thus to represent a younger generation of crystal growth (e.g. Fig. 3c, d). The Group AB, B, C, BC and D samples show highly variable whole-rock compositions compared to Group A harzburgites (Fig. 8). These chemical variations are robust evidence of metasomatism. The textural and chemical data thus imply that the upper mantle beneath Fuerteventura has a complex evolutionary history.

7.1. Oceanic lithospheric mantle beneath Fuerteventura

The cores of olivine and orthopyroxene porphyroclasts in Group A (and AB) harzburgites, which represent the oldest petrographic features, cover narrow ranges in compositions that fall within, or close to, the depleted parts of the fields covered by minerals in mantle peridotites recovered in the MARK area along the central part of the Mid-Atlantic Ridge (Figs. 4 and 5). This is also true for clinopyroxene and spinel in Group A harzburgites (Figs. 6 and 7). With respect to whole-rock compositions Group A harzburgites have lower SiO_2 and higher Na_2O contents than those found among average depleted Mid-Atlantic Ridge (MAR) peridotites (based on data from Myashiro et al. (1979), Michael and Bonatti (1985), Cannat et al. (1995), Casey (1997), Stephens (1997), Brandon et al. (2000) and Lee et al. (2003), whereas the contents of other major elements fall within, or close to, the high-mg# part of the MAR peridotite field (Fig. 8). Furthermore, the compositions of the Group A harzburgites and their minerals are closely similar to spinel harzburgites from Lanzarote (Figs. 4–7). The position of the whole rock compositions of Group A harzburgites in Fig. 8 indicates that the initial composition of the mantle lithosphere beneath Fuerteventura (as of that beneath Lanzarote) resembles that of the most refractory peridotites retrieved along the Mid-Atlantic Ridge.

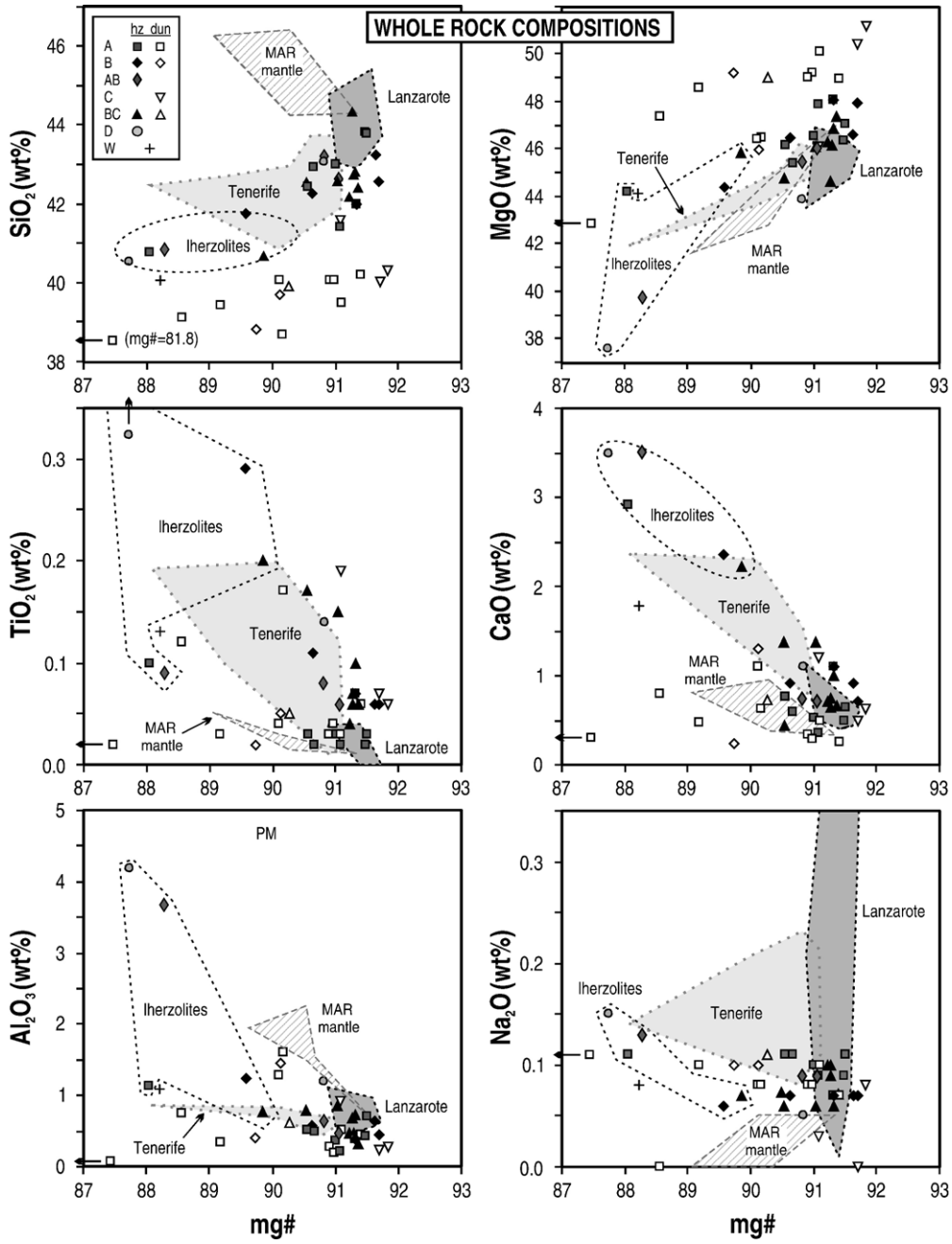

Fig. 8. Whole-rock variations of major oxides (wt.%) plottet against mg# for mantle xenoliths from Fuerteventura. The data are compared to strongly depleted spinel harzburgites from Lanzarote (Neumann et al., 1995), depleted to strongly metasomatized harzburgites and lherzolites from Tenerife (Neumann et al., 2002), and average peridotites collected along different parts of the Mid-Atlantic Ridge (based on data from Myashiro et al., 1979; Michael and Bonatti, 1985; Cannat et al., 1995; Casey, 1997; Stephens, 1997; Brandon et al., 2000; Lee et al., 2003). See text for discussion.

Previous studies have concluded that the upper mantle beneath the Canary Islands (La Palma, Hierro, Tenerife and Lanzarote) represents old oceanic lithosphere that has suffered different degrees of metasomatism (e.g. Neumann, 1991; Neumann et al., 1995, 2002, 2004). The spinel harzburgites from Lanzarote have been only very mildly affected by metasomatic processes, thus being chemically close to the original composition of the oceanic mantle lithosphere beneath the Canary Islands (Neumann et al., 2004). Our results imply that also the lithospheric mantle beneath Fuerteventura represents old oceanic lithospheric mantle

whose original major element composition is essentially preserved in the Group A harzburgites. The xenoliths belonging to the other textural groups represent parts of the lithospheric mantle that have been texturally and chemically modified after initial formation.

7.2. The formation of "fibrous textures"

We showed above that the primary textures in the Fuerteventura xenoliths have been modified to various degrees by the development of "fibrous textures" (Fig. 3b–f). Evidence of incongruent melting in some samples (local replacement of fibrous orthopyroxene by ol + glass ± sp; Fig. 3e) indicates that the formation of fibrous orthopyroxene took place before entrainment of the xenoliths in the host magmas. Also the overall mode of occurrence of the fibrous textures indicates an early origin. The textural relationships imply that the formation of the "fibrous textures" must have involved more than one stage, the net result of which is partial break-down of both orthopyroxene and olivine porphyroclasts (Fig. 3b–d), formation of new (fibrous) orthopyroxene at the expense of both olivine and orthopyroxene, and growth of olivine at the expense of orthopyroxene (indicated by parallel rows or minute spinel inclusions in irregular olivine inside recrystallized domains, and in the rims of olivine porphyroclasts along recrystallized domains; Fig. 3e). The porous nature of the fibrous orthopyroxene domains, the spongy olivine rims, and of other fine-grained aggregates (Fig. 3f) implies that these domains have contained significant volumes of fluids.

The nature of the processes leading to the formation of "fibrous textures" in the upper mantle beneath Fuerteventura is not obvious. Fibrous orthopyroxene has been described elsewhere, for example in peridotite xenoliths in the Avacha volcano in the Kamchatka Arc, Russia (Arai et al., 2003), and in partly serpentinized ultramafic rocks belonging to the Nevado–Filábride Complex in the Cordillas Béticas in SE Spain (Trommsdorff et al., 1998). Arai et al. (2003) interpreted the recrystallization to fibrous orthopyroxene observed in mantle xenoliths in the Avacha volcano as the results of metasomatic reactions involving a silicic hydrous fluid or melt. Dissolution of primary olivine and orthopyroxene, and formation of secondary fibrous orthopyroxene due to fluid interaction with the mantle wedge have also been documented in the Lihir sub-arc peridotites (McInnes et al., 2001). Trommsdorff et al. (1998) interpreted the textures in rocks in SE Spain as the results of prograde, high pressure transitions from antigorite serpentinite to enstatite–olivine rocks. Similar models have been presented by e.g. Smith et al. (1999), and Arai and Kida (2000). Radial fibrous orthopyroxene aggregates, similar to those observed in some Fuerteventura samples (FBA1-1 and FBA1-3), are common in deserpentinized peridotite in contact metamorphic aureoles (e.g. Arai, 1974, 1975; Matsumoto et al., 1995; Arai and Kida, 2000). Our data on mantle xenoliths with "fibrous textures" must thus be tested against two models: (1) metasomatic reactions between peridotite wall-rocks and infiltrating hydrous fluids or melts, and (2) heating and dehydration of partly serpentinized peridotites.

The formation of "fibrous textures" in the upper mantle beneath Fuerteventura as the results of interaction with a metasomatic (hydrous) fluid or melt is possible. Studies of mantle xenoliths from the other Canary Islands have shown that a series of liquids and fluids have been in operation in the upper mantle beneath the Canary Islands, including basaltic melts, high-Si melts ($SiO_2 > 60$ wt.%), ultramafic silicate melts, carbonatitic melts, CO_2-rich fluids and H_2O–NaCl brine (Hansteen et al., 1991; Frezzotti et al., 1994, 2002a,b; Neumann et al., 1995, 2002). However, none of the highly metasomatized rocks from other islands show fibrous textures. Furthermore, most of the Fuerteventura samples with fibrous textures cover a relatively restricted mg#-range, whereas progressive metasomatism in the other islands (exemplified in Fig. 8 by the Tenerife field) typically is expressed by decreasing mg# (and increasing TiO_2 and CaO). The lherzolite xenoliths from Fuerteventura fall on the Tenerife metasomatic trend, but not the harzburgites with fibrous textures. The lowest mg# and highest CaO contents among the Fuerteventura harzburgites and lherzolites are actually found in Group A and AB lherzolites where fibrous textures are absent or rare. We therefore believe the formation of fibrous textures and the metasomatism to have formed by different processes. Also reactions with H_2O–NaCl brines seem unlikely in light of the tendency for xenoliths with "fibrous textures" tend to have lower Na_2O contents than peridotites without "fibrous textures" from both Fuerteventura (Group A; Fig. 8) and the other islands. Finally, the complex nature of the "fibrous textures" implies that if they have been formed by metasomatism, at least two metasomatic agents must have been in operation in order to account for the evidence of periods of undersaturation and saturation in both orthopyroxene and olivine. However, the possibility that the "fibrous textures" formed as the result of metasomatic reactions cannot be discarded on the basis of the data available so far.

Serpentinization is supposed to be common in the oceanic mantle lithosphere, and may occur close to the mid-ocean ridge, along fracture zones and in continent–ocean transition zones (e.g. Cannat, 1993, 1996; Reston et al., 2001). Serpentinized peridotites might therefore be expected in the upper mantle beneath the Canary Islands. We have found spinel harzburgites with fibrous orthopyroxene domains (similar to those exhibited by Group B in Fuerteventura) in mantle xenoliths from Lanzarote, but "fibrous textures" have not been observed in mantle xenoliths from any of the other Canary Islands. The fact that "fibrous textures" have only been observed in xenoliths from the easternmost islands, Lanzarote and Fuerteventura, suggests that their formation may be caused by processes associated with the continent–ocean transition, such as serpentinization. We show below that partial serpentinization followed by dehydration due to heating during the Canary Islands magmatism may account for the complex textural relationships exhibited by the mantle xenoliths from Fuerteventura.

Most of the peridotite xenoliths in Fuerteventura have mg#>90, and they consist mainly of olivine and orthopyroxene. Information about potential serpentinization in such rocks may be demonstrated in the $MgO–SiO_2–H_2O$ system. The harzburgites, lherzolites and dunites discussed here, like oceanic peridotites in general, are significantly richer in olivine than in orthopyroxene and plot along the ol–opx tie-line relatively close to olivine in Fig. 9. In our example, we assume a rock, R, consisting of about 80% olivine and 20% orthopyroxene. With increasing addition of H_2O, olivine and orthopyroxene are progressively broken down to antigorite (and/or chlorite) as the bulk-rock composition is shifted along a straight line towards the H_2O-corner (Fig. 9). The rock eventually reaches the olivine+antigorite/chlorite (ol+ant/chl) tie-lie, at which stage all the orthopyroxene plus almost half of the olivine have been serpentinized, and the water-saturated rock consists of olivine and antigorite and/or chlorite. With additional water the rock becomes water-oversaturated and enters the ol+ant/Chl+H_2O field, where serpentinization of olivine progresses. The stable phase assemblages in the Fuerteventura xenoliths under H_2O-saturated conditions have been tested by the Perple_X program developed by James Connolly (www.perplex.ethz.ch) with the Perplith modification developed by Boris Kaus (www.geology.ethz.ch/sgt/staff/boris/perplith.htm), which compute pressure–temperature phase diagram sections for systems with constrained compositions. The phase diagrams obtained for the major element compositions of

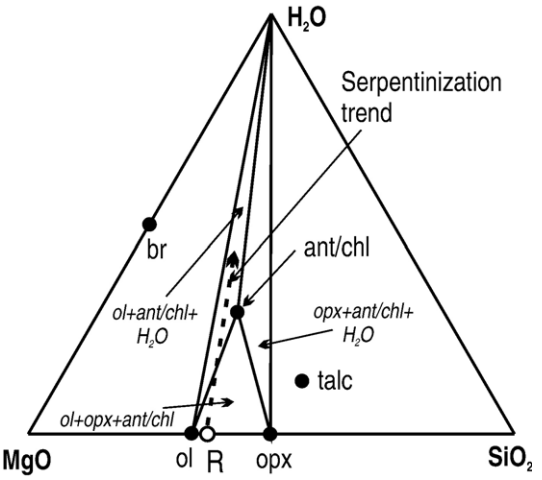

Fig. 9. Phase relationships in the system $MgO–SiO_2–H_2O$ (molecular proportions). The dashed arrow demonstrates that progressive serpentinization of a typical harzburgite (R) consisting of 80% olivine (ol) and 20% orthopyroxene (opx) from Fuerteventura will lead to complete consumption of orthopyroxene (opx) while there is still considerable amounts of olivine (ol) in the rock. *Ant:* antigorite, *chl:* chlorite, *br:* brucite. See text for discussion.

the Fuerteventura harzburgites and lherzolites show complete break-down of orthopyroxene at temperatures between about 900 and 700 °C. One of the phase diagrams (Group C harzburgite FBA1-4) computed by Perple_X-Perplith is shown in Fig. 10. The low-temperature limits for complete consumption of orthopyroxene in samples FU9-8 (Group BC harzburgite) and FBA1-22 (Group B harzburgite) are shown as dashed lines. Heating of partly serpentinized peridotite would reverse the processes, causing replacement of the hydrous phases by orthopyroxene, olivine and clinopyroxene. Partial serpentinization followed by heating and dehydration may thus account for the complex petrographic relationships exhibited by the mantle xenoliths from Fuerteventura.

There is one possible problem with the serpentinization model. Orthopyroxenes formed at the expense of serpentine have been found to have lower CaO, Al_2O_3, and Cr_2O_3 than primary orthopyroxene in coexisting rocks (e.g. Arai, 1974, 1975; Springer, 1974; Arai and Kida, 2000). This is not true for the fibrous orthopyroxene in the mantle xenoliths from Fuerteventura. In these rocks the fibrous orthopyroxene partly have lower, partly similar CaO, Al_2O_3, Cr_2O_3 contents compared to the orthopyroxene porphyroclasts (Fig. 5). However, the orthopyroxene in the Fuerteventura xenoliths is generally depleted in Al_2O_3, CaO and Cr_2O_3 relative to orthopyroxene in oceanic peridotites (e.g. in the MARK area; Fig. 5). It should also be noticed that the xenoliths have been subjected to metasomatism

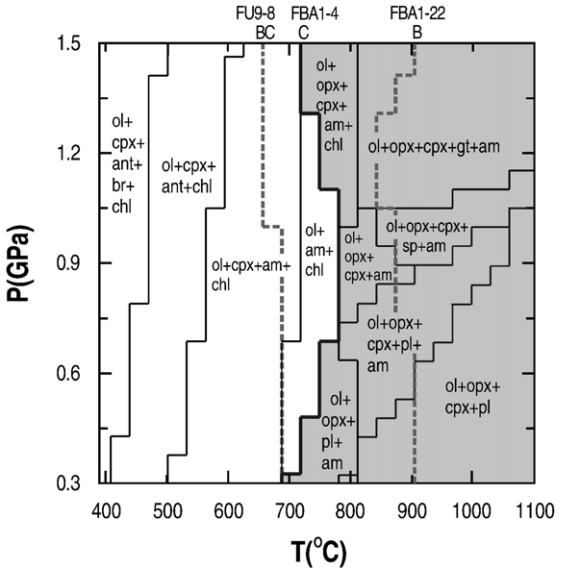

Fig. 10. Pressure–temperature phase diagram sections for a H_2O-saturated systems with FBA1-4 (Group C) composition computed by the Perple_X program (James Connolly) with Perplith modification (Boris Kaus). The grey field shows P–T conditions at which orthopyroxene is stable, the white field the conditions where all orthopyroxene (and some olivine) has been consumed by serpentinization. Heavy dashed lines show the lower P–T limits for orthopyroxene in H_2O-saturated systems with rock compositions corresponding to FT9-8 (Group BC) and FBA1-22 (Group B). Computations indicate that at pressures expected in the oceanic lithospheric mantle, progressive serpentinization would lead to total consumption of orthopyroxene in mantle xenoliths from Fuerteventura at temperatures below ca. 650 °C. *Ol:* olivine, *opx:* orthopyroxene, *cpx:* clinopyroxene, *gt:* garnet, *am:* amphibole, *sp:* spinel, *pl:* plagioclase, *chl:* chlorite, *ant:* antigorite, *br:* brucite. See text for discussion.

with addition of CaO and other chemical components (see discussion below).

In conclusion, we consider moderate serpentinization, followed by heating during the formation of Fuerteventura, to be the most likely mode of formation of the "fibrous textures" (both the fibrous orthopyroxene and spongy rims and stringy inclusion trails in olivine) exhibited by many mantle xenoliths from Fuerteventura. The observed differences in textural types, and different proportions of "fibrous textures", may be explained by local serpentinization along faults and fractures, leaving parts of the mantle untouched. Bonatti et al. (1986) have described serpentinization along a fault zone in the island of Zabargad in the Red Sea, whereas the peridotites in other parts of the island generally are very fresh. Different modal assemblages of the initial rocks (particularly different proportions of orthopyroxene to olivine), would cause variations in the types of "fibrous textures" that were formed.

Serpentinized peridotites have been recovered in the rift-valleys of slow-spreading ridges, in fracture zones (e.g. Minshull et al., 1998), as well as in continent–ocean transition zones (e.g. Whitmarsh et al., 2001). Our results imply that if serpentinization has taken place in the lithosphere beneath the Canary Islands, it is restricted to the close vicinity of the original break-up zone between the easternmost Canary Islands and the African continent (Fig. 1). This is in agreement with the general belief that the continent–ocean transitions of non-volcanic rifted margins tend to be tectonically unstable and may be cut by faults and fractures penetrating into the upper mantle, thus forming potential pathways for seawater to invade the upper mantle and cause serpentinization (e.g. Minshull et al., 1998).

The most likely cause of dehydration is heating during the Canary Islands magmatic event. The small grain-size of the fibrous domains and the range in mineral compositions seen at the scale of a thin-section indicates that they have not had time to grow to larger grain-size or to reach chemical equilibrium.

7.3. Metasomatism

The wide range in chemical compositions exhibited by the mantle xenoliths from Fuerteventura indicates that parts of the underlying upper mantle has been chemically modified (Fig. 8). The chemical modification involves addition of Ti, Al, Fe, Ca, and CO_2, and reactions leading to the crystallization of clinopyroxenes and carbonates (and other phases). Evidence of metasomatism is also seen in the following: clinopyroxenes, spinel and whole-rock compositions tend to be highly enriched in Ti, Fe^{3+} and Na relative to MAR peridotites (Figs. 6–8). There is a tendency for higher Fe in neoblasts and rims of porphyroclasts in olivines and orthopyroxenes than in the cores of porphyroclasts (Tables 1 and 2, Fig. 4). This is also true for Group A harzburgites. Furthermore, many xenoliths are significantly richer in Ca than are MAR peridotites. Finally, like strongly metasomatized xenoliths from the other Canary Islands, many harzburgites and lherzolites from Fuerteventura have lower SiO_2 contents than MAR peridotites; the lherzolites have lower SiO_2 concentrations and mg# ratios, as well as higher CaO than the MAR peridotites (Fig. 8). As indicated above, these deviations from MAR peridotite compositions, which are most strongly expressed in the lherzolites, are seen among all the Fuerteventura xenolith groups, including Group A xenoliths which lack "fibrous textures", and are thus clearly not the results of the serpentinization–

dehydration processes. Instead, we attribute these chemical features to metasomatism caused by interaction between mantle wall-rocks and melts and/or fluids associated with the Canary Islands magmatism. This does not mean that the serpentinization–dehydration processes did not involve mobilization of chemical components other than H_2O, on the contrary. It is well known that many oxides are highly soluble in water, particularly in hot water (e.g. Si, Ca, Na and K; e.g. Henderson, 1982). However, it is difficult to distinguish between mobilization of elements due to hydration–dehydration and to metasomatism caused by other agents. We find the fact that the Fuerteventura samples whose compositions deviate most strongly from the MAR peridotite field overlap with, or even fall in the extensions of, the Tenerife trends to be strong evidence that similar metasomatic agents have affected the upper mantle beneath both these islands. There is, however, one interesting difference between mantle xenoliths from Fuerteventura and the other Canary Islands. It has formerly been found that a large proportion of the xenoliths which represent highly metasomatized upper mantle beneath the Canary Islands (Tenerife and La Palma), tend to carry small amounts of phlogopite (mainly in fluid inclusions), whereas phlogopite is generally absent from xenoliths from mildly metasomatized mantle domains. Although the lherzolites from Fuerteventura appear to have been strongly metasomatized, no phlogopite has been observed. The lack of phlogopite may be a result of heating and partial melting during ascent.

Metasomatism in the upper mantle beneath Tenerife has been discussed in detail by Frezzotti et al. (2002a) and Neumann et al. (2002). Based on the results from Tenerife, we propose that the high CaO and low SiO_2 concentrations exhibited by harzburgites and lherzolites from Fuerteventura most likely reflect reactions between melts and harzburgite wall-rocks leading to the formation of olivine+clinopyroxene+Si-rich melt at the expense of orthopyroxene; the lherzolites are thus formed from harzburgites by extensive metasomatic reactions. Glass inclusions and interstitial glasses with SiO_2 contents in the range 60–70 wt.% are common in mantle xenoliths from Fuerteventura as in mantle xenoliths from the other Canary Islands (e.g. Wulff-Pedersen et al., 1996; Neumann and Wulff-Pedersen, 1997; Neumann et al., 2002). Similar silicic glass inclusions and interstitial glasses are present in mantle xenoliths from Fuerteventura (Abu El-Rus and Neumann, 2005, unpublished data). The metasomatism has most likely been caused in situ in the mantle by fluids and melts percolating through the upper mantle during the formation of Fuerteventura. However, some effects of interaction with the host magmas during ascent cannot be excluded. This may particularly be true for the fine-grained Group D sample FBA1-23 that is highly enriched in TiO_2, Al_2O_3 and CaO, and contains a lot of interstitial glass.

7.4. Formation of the dunites (and wehrlite)

Dunites in the mantle are generally envisioned as: (1) residues of very high degrees of partial melting (e.g. Jackson and Ohenstetter, 1981), (2) products of reactions between olivine-saturated magmas and mantle wall-rocks (e.g. Quick, 1981; Nicolas, 1986; Kelemen, 1990; Kelemen et al., 1995, 1998), or (3) olivine 'cumulate' dykes (fractures in the lithospheric mantle filled with olivine precipitated by ascending melt (e.g. Nicolas and Jackson, 1982; Sen and Presnall, 1986; Takahashi, 1992; Suhr et al., 1998). For simplicity we include the wehrlite FT9-15 in the discussion below.

With the exception of fibrous orthopyroxenes which are rare in the dunites, the textures of the dunites are similar to those of the harzburgites (including the low-mg# sample FT9-4), and their olivine porphyroclasts (with the exception of sample FT9-4; Fig. 4) fall within the same mg# and NiO ranges as those in the harzburgites. However, there are also significant compositional differences between the dunites (and wehrlite) and the harzburgites. The dunites tend towards lower whole-rock mg# (Fig. 8), in many dunites the clinopyroxenes have significantly higher TiO_2 and Al_2O_3 than those in harzburgites and lherzolites (Fig. 6), and their spinels (particularly rims and symplectites) have significantly higher Fe^{2+} and Fe^{3+} (Fig. 7; Table 4). Furthermore, whereas modeling predicts decreasing SiO_2 with increasing MgO with progressive partial melting (e.g. Niu et al., 1997), the dunites from Fuerteventura show decreasing SiO_2 with decreasing MgO (Fig. 8). An additional important point is that the dunites contain clinopyroxene and no, or little, orthopyroxene. These chemical characteristics imply that the dunites do not represent residues formed by very high degrees of partial melting. Progressive partial melting of lherzolite or harzburgite is expected to remove clinopyroxene well before the exhaustion of orthopyroxene (e.g. Jaques and Green, 1980). The textures and chemical variations among the dunites strongly suggest reactions between mantle wall-rocks and silica-undersaturated melts in equilibrium with olivine and clinopyroxene, and relatively high Fe^{3+}/Fe^{2+} ratios. Fe–Ti enrichment in the mantle is commonly attributed to the interaction with basaltic melts (e.g. Wilshire et al.,

1980; Harte, 1983, Schneider and Eggler, 1986; Wilshire, 1987; Neumann, 1991). It thus seems possible that some of the dunites formed by interaction between the mantle wall-rocks and basaltic Canary Islands magmas. However, many dunites combine mg#<90 with relatively low TiO_2 concentrations (Fig. 8). It therefore seems likely that the dunites result from reactions between mantle wall-rocks and melts of different compositions.

The wehrlite shows affinity to the lherzolites and dunites with respect to whole-rock and mineral chemistry, but exhibits cumulate textures. It seems likely that this rock represents a cumulate formed from basaltic melts ascending through the mantle.

8. Conclusions

Mantle xenoliths collected from Holocene volcanic cones in northern Fuerteventura comprise highly refractory spinel harzburgites and spinel dunites, together with rare spinel lherzolites and spinel wehrlite. The mineral assemblage are ol ± opx ± sp ± cpx, clinopyroxene occurs only as neoblasts; hydrous phases have not been observed. The xenoliths exhibit a wide range of textures from protogranular and porphyroclastic to fine-grained, and commonly contain domains of fibrous orthopyroxene, mottled rims on olivine, and poorly to well developed networks of fluid inclusion trails and trails of fibrous material criss-crossing olivine porphyroclasts. Petrographic observations together with mineral and whole-rock chemistry suggest the following evolutionary history of the lithospheric mantle beneath Fuerteventura:

(1) The mantle rocks that became accreted to the oldest oceanic crust outside Morocco was highly refractory due to melt extraction, with a composition similar to that of the most refractory peridotites collected along the Mid-Atlantic Ridge.
(2) At some later stage the mantle was locally invaded by sea-water. This led locally to moderate serpentinization.
(3) Textures reflecting former serpentinization have only been found in xenoliths in Fuerteventura and in rare xenoliths from Lanzarote, which are the two easternmost Canary Islands. It therefore seems likely that serpentinization occurred locally along deep faults and fractures caused by instability along the continent–ocean transition.
(4) Heating of the lithosphere during the Fuerteventura magmatism caused dehydration of partly serpentinized mantle rocks, replacing hydrous minerals by domains of fibrous, porous orthopyroxene, and new growth of olivine.
(5) The serpentinization and dehydration processes clearly involved chemical exchange between mantle minerals and hydrous fluids, including sea-water.
(6) During the Canary Islands magmatism the upper mantle beneath Fuerteventura also suffered metasomatism by, and reactions with, melts and fluids, leading to decreased SiO_2, and addition of Fe^{2+} and Fe^{3+}, Ca, and Na, locally also Ti and Al.
(7) The dunites, lherzolites and wehrlites are the products of extensive metasomatic processes involving both basaltic melts and melts of other compositions.
(8) During ascent with the host magma, many xenoliths suffered beginning partial melting induced by decompression and heating. This is seen in melt pockets with microphenocrysts, and may also be reflected in spongy rims on granular Cr-spinel, and melt pockets with euhedral to subhedral olivine grains within the fibrous domains.

Acknowledgements

Most of this work was carried out at the Geology Department, Oslo University, Norway during M.M.A.A. E's tenure of a scholarship from The Research Council of Norway for project title "The upper mantle beneath Fuerteventura, the easternmost Canary Island". The project is supported by grants from the Norwegian Research Council for Science and Humanities (NAVF) to ERN. We are indebted to James Connolly and Boris Kaus for information about Perple_X-Perplith program (www.perplex.ethz.ch and www.geology.ethz.ch/sgt/staff/boris/perplith.htm), and to Stefan Schmalholst for help with these programs. We are also indebted to Bjørn Jamtveit for enlightening discussions on serpentinization. Muriel Erambert has given invaluable help with the microprobe analyses. The paper has improved through the constructive criticism by two anonymous reviewers.

References

Abdel-Monem, A., Watkins, N.D., Gast, P.W., 1971. Potassium–argon ages, volcanic stratigraphy, and geomagnetic polarity history of the Canary Islands: Lanzarote, Fuerteventura, Gran Canaria, and La Gomera. American Journal of Science 271, 490–521.

Abdel-Monem, A., Watkins, N.D., Gast, P.W., 1972. Potassium–argon ages, volcanic stratigraphy, and geomagnetic polarity history of the Canary Islands: Tenerife, La Palma, and Hierro. American Journal of Science 272, 805–825.

Arai, S., 1974. 'Non-calciferous' orthopyroxene and its bearing in the petrogenesis of ultramafic rocks in Sangun and Joetsu zones. Journal of Japanese Association of Mineralogists, Petrologists and Economic Geologists 69, 343–353.

Arai, S., 1975. Contact metamorphosed dunite–harzburgite complex in the Chugoku district, western Japan. Contributions to Mineralogy and Petrology 51, 1–16.

Arai, S., Kida, M., 2000. Origin of fine-grained peridotites xenoliths from Iraya volcano of Batan Island, Philippines: deserpentinization or metasomatism at wedge mantle beneath an incipient arc? Island Arc 9, 458–471.

Arai, S., Ishimaru, S., Okrugin, V.M., 2003. Metasomatized harzburgite xenoliths from Avacha volcano as fragments of mantle wedge of the Kamchatka arc: implication for the metasomatic agent. Island Arc 12, 233–246.

Balogh, K., Ahijado, A., Casillas, R., Fernandez, C., 1999. Contributions to the chronology of the Basal Complex of Fuerteventura, Canary Islands. Journal of Volcanology and Geophysical Research 90, 81–101.

Bonatti, E., Ottonello, G., Hamlyn, P.R., 1986. Peridotites from the island of Zabargad (St. John), Red Sea; petrology and geochemistry. Journal of Geophysical Research 91, 599–631.

Brandon, A.D., Snow, J.E., Walker, R.J., Morgan, J.W., Mock, T.D., 2000. ^{190}Pt–^{186}Os and ^{187}Re–^{187}Os systematics of abyssal peridotites. Earth and Planetary Science Letters 177, 319–335.

Cannat, M., 1993. Emplacement of mantle rocks in the seafloor at mid-ocean ridges. Journal of Geophysical Research 98, 4163–4172.

Cannat, M., 1996. How thick is the magmatic crust at slow spreading oceanic ridges? Journal of Geophysical Research 101, 2847–2857.

Cannat, M., Karson, J.A., Miller, D.J., Agar, S.M., Barling, J., Casey, J.F., Ceuleneer, G., Dilek, Y., Fletcher, J., Fujibayashi, N., Gaggero, L., Gee, J.S., Hurst, S.D., Kelley, D.S., Kempton, P.D., Lawrence, R.M., Marching, V., Mutter, C., Niida, K., Rodway, K., Ross, D.K., Stephens, C., Werner, C.D., Whitechurch, H., Fox, C.O.Proccedings of the Ocean Drilling Program, Part A: Initil Report, vol. 153, pp. 259–274.

Casey, J.F., 1997. Composition of major- and trace-element geochemistry of abyssal peridotites and mafic plutonic rocks with basalts from the MAR region of the Mid-Atlantic Ridge. In: Karson, J.A., Cannat, M., Miller, D.J., Elthon, D. (Eds.), Proceedings of the Ocean Drilling Program, Scientific Results, vol. 153, pp. 181–241.

Coello, J., Cantagrel, J.M., Hernan, F., Fúster, J.M., Ibarrola, E., Ancochea, E., Casquet, C., Jamond, C., Diaz, T.J.R., Cendrero, A., 1992. Evolution of the eastern volcanic ridge of the Canary Islands based on new K–Ar data. Journal of Volcanology and Geothermal Research 53, 251–274.

Frey, F.A., Prinz, M., 1978. Ultramafic inclusions from San Carlos, Arizona: petrologic and geochemical data bearing on their petrogenesis. Earth and Planetary Science Letters 38, 129–176.

Frezzotti, M.L., Touret, J.L.R., Lustenhouwer, W.J., Neumann, E.-R., 1994. Melt and fluid inclusions in dunite xenoliths from La Gomera, Canary Islands: tracking the mantle metasomatic fluids. European Journal of Mineralogy 6, 805–817.

Frezzotti, M.L., Andersen, T., Neumann, E.-R., Simonsen, S.L., 2002a. Carbonatite melt-CO_2 fluid inclusions in mantle xenoliths from Tenerife, Canary Islands: a story of trapping, immiscibility and fluid–rock interaction in the upper mantle. Lithos 64, 77–96.

Frezzotti, M.L., Touret, J.L.R., Neumann, E.-R., 2002b. Ephemeral carbonatite melts in the upper mantle: carbonatite–silicate immiscibility in microveins and inclusions within spinel peridotite xenoliths, La Gomera, Canary Islands. European Journal of Mineralogy 14, 891–904.

Fúster, J.M., Cendrero, A., Gastesi, P., Ibarrola, E., Lopez Ruiz, J., 1968. Geologíla y volcanología de las isles Canarias-Fuerteventura. Instituto "Lucas Mallada". Consejo Superior de Investigaciones Científicas, Madrid. 239 pp.

Hansteen, T.H., Andersen, T., Neumann, E.-R., Jelsma, H., 1991. Fluid and silicate melt inclusions in spinel lherzolite xenoliths from Hierro, Canary Islands: Implications for mantle metasomatism. Contributions to Mineralogy and Petrology 107, 242–254.

Harte, B., 1983. Mantle peridotites and processes; the kimberlite sample. In: Hawkesworth, C.J., Norry, M.J. (Eds.), Continental Basalts and Mantle Xenoliths; Papers Prepared for a UK Volcanic Studies Group Meeting at the University of Leicester, pp. 46–91.

Henderson, P., 1982. Inorganic Geochemistry. Pergamon Press, Oxford. 353 pp.

Henry, D.J., Medaris, L.G., 1980. Application of pyroxene and olivine-spinel geothermometers to spinel peridotites in southwestern Oregon. American Journal of Science 280A, 211–231.

Hoernle, K., 1998. Geochemistry of Jurassic oceanic crust beneath Gran Canaria (Canary Islands): implications for crustal recycling and assimilation. Journal of Petrology 39, 859–880.

Jackson, M., Ohenstetter, M., 1981. Peridotite and gabbroic structures in the Monte Maggiore massif, Alpine Corsica. Journal of Geology 89, 703–719.

Jaques, A.L., Green, D.H., 1980. Anhydrous melting of peridotite at 0–15 kb pressure and the genesis of tholeiitic basalts. Contributions to Mineralogy and Petrolology 73, 287–310.

Kelemen, P.B., 1990. Reaction between ultramafic rock and fractionating basaltic magma: I. Phase relations, the origin of calc-alkaline magma series, and the formation of discordant dunite. Journal of Petrology 31, 51–98.

Kelemen, P.B., Shimizu, N., Salters, V.J.M., 1995. Extraction of mid-ocean-ridge basalt from the up-welling mantle by focused flow of melt in dunite channels. Nature 375, 347–753.

Kelemen, P.B., Hart, S.R., Bernstein, S., 1998. Silica enrichment in the continental upper mantle via melt/rock reaction. Earth and Planetary Science Letters 164, 387–406.

Komor, S.C., Grove, T.L., Hébert, R., 1990. Abyssal peridotites from ODP Hole 670A (21(10N, 45(02W): residues of mantle melting exposed by non-constructive axial divergence. In: Detrick, R., Honnorez, J., Bryan, W.B., Juteau, T., et al., (Eds.), Proceedings of the Ocean Drilling Program, Scientific Results, vol. 106/109, pp. 85–99.

Le Bas, M.J., Rex, D.C., Stillman, C.J., 1986. The early magmatic chronology of Fuerteventura. Geological Magazine 123, 287–298.

Lee, C.-T., Brandon, A.D., Norman, M., 2003. Vanadium in peridotites as a proxy for paleo-fO_2 during partial melting: prospects, limitations, and implications. Geochimica et Cosmochimica Acta 67, 3045–3064.

Matsumoto, I., Arai, S., Muraoka, H., Yamauchi, H., 1995. Petrological characteristics of dunite–harzburgite–chromitite complexes of the Sangun zone, Southwest Japan. Journal of Mineralogy, Petrology and Economic Geology 90, 13–26.

McInnes, B.I.A., Gregoire, M., Binns, R.A., Herzig, P.M., Hannington, M.D., 2001. Hydrous metasomatism of oceanic sub-arc mantle, Lihir. Papua New Guinea: petrology and geochemistry of fluid-metasomatised mantle wedge xenoliths. Earth and Planetary Science Letters 188, 169–183.

Mercier, J.-C.C., Nicolas, A., 1975. Textures and fabrics of upper mantle peridotites as illustrated by basalt xenoliths. Journal of Petrolology 16, 454–487.

Michael, P.J., Bonatti, E., 1985. Peridotite composition from the North Atlantic; regional and tectonic variations and implications for partial melting. Earth and Planetary Science Letters 73, 91–104.

Minshull, T.A., Muller, M.R., Robinson, C.J., White, R.S., Bickle, M.J., 1998. Is the oceanic Moho a serpentinization front? In: Mills, R.A., Harrison, K. (Eds.), Modern Oceanic Floor Processes and the Geological Record, Geological Society, London, Special Publications, vol. 148, pp. 71–80.

Myashiro, A., Shido, F., Kanehira, K., 1979. Metasomatic chloritization of gabbros in the Mid-Atlantic Ridge near 30 degrees N. Marine Geology 31, M47–M52.

Neumann, E.-R., 1991. Ultramafic and mafic xenoliths from Hierro, Canary Islands: evidence for melt infiltration in the upper mantle. Contributions to Mineralogy and Petrology 106, 236–252.

Neumann, E.-R., Wulff-Pedersen, E., 1997. The origin of highly silicic glass in mantle xenoliths from the Canary Islands. Journal of Petrology 38, 1513–1539.

Neumann, E.-R., Wulff-Pedersen, E., Johnsen, K., Andersen, T., Krogh, E., 1995. Petrogenesis of spinel harzburgite and dunite suite xenoliths from Lanzarote, eastern Canary Islands: implications for the upper mantle. Lithos 35, 83–107.

Neumann, E.-R., Wulff-Pedersen, E., Pearson, N., Spencer, E.A., 2002. Mantle xenoliths from Tenerife (Canary Islands): evidence for reactions between mantle peridotites and silicic carbonatite melts inducing Ca Metasomatism. Journal of Petrology 43, 825–857.

Neumann, E.-R., Griffin, W.L., Normann, J.P., O'Reilly, S.Y., 2004. The evolution of the upper mantle beneath the Canary Islands: information from trace elements and Sr isotope ratios in minerals in mantle xenoliths. Journal of Petrology 45, 2573–2612.

Nicolas, A., 1986. A melt extraction model based on structural studies in mantle peridotites. Journal of Petrology 27, 999–1022.

Nicolas, A., Jackson, M., 1982. High temperature dikes in peridotites: origin by hydraulic fracturing. Journal of Petrology 23, 568–582.

Niida, K., 1997. Mineralogy of MARK peridotites: replacement through magma channelling examined from Hole 920D, MARK area. In: Karson, J.A., Cannat, M., Miller, D.J., Elthon, D. (Eds.), Proceedings of the Ocean Drilling Program, Scientific Results, vol. 153, pp. 265–275.

Niu, Y., Langmuir, C.H.., Kinzler, R., 1997. The origin of abyssal peridotites: a new perspective. Earth and Planetary Science Letters 152, 251–265.

Quick, J.E., 1981. The origin and significance of large, tabular dunite bodies in the Trinity peridotite, Northern California. Contributions to Mineralogy and Petrology 78, 413–422.

Reston, T.J., Pennell, J., Stubenrauch, A., Walker, I., Perez-Gussinya, M., 2001. Detachment faulting, mantle serpentinization, and serpentinite-mud volcanism beneath the porcupine Basin, southwest of Ireland. Geology 29, 587–590.

Roedder, E., 1984. Fluid inclusions. Reviews in Mineralogy, Mineralogical Society of America 12. 643 pp.

Roest, W.R., Dañobeitia, J.J., Verhoef, J., Collette, B.J., 1992. Magnetic anomalies in the Canary Basin and the Mesozoic evolution of the central North Atlantic. Marine Geophysical Researches 14, 1–24.

Ross, K., Elthon, D., 1997. Extreme incompatible trace-element depletion of diopside in residual mantle from south of the Kane Fracture Zone. In: Karson, J.A., Cannat, M., Miller, D.J., Elthon, D. (Eds.), Proceedings of the Ocean Drilling Program, Scientific Results, vol. 153, pp. 277–284.

Schneider, M.E., Eggler, D.H., 1986. Fluids in equilibrium with peridotite minerals: implications for mantle metasomatism. Geochimica et Cosmochimica Acta 50, 711–724.

Schmincke, H.-U., 1982. Volcanic and chemical evolution of the Canary Islands. In: von Rad, U., Hinz, K., Sarnthein, M., Seibold, E. (Eds.), Geology of the Northwest African Continental Margin. Springer, Berlin, pp. 274–306.

Schroeder, T., John, B., Frost, B.R., 2002. Geologic implication of seawater circulation through peridotite exposed at slow-spreading mid-ocean ridges. Geology 30, 367–370.

Sen, G., Presnall, D.C., 1986. Petrogenesis of dunite xenoliths from Koolau Volcano, Oahu, Hawaii: Implications for Hawaiian volcanism. Journal of Petrology 27, 197–217.

Siena, F., Beccaluva, L., Coltorti, M., Marchesi, S., Morra, V., 1991. Ridge to hot-spot evolution of the Atlantic lithospheric mantle: evidence from Lanzarote peridotite xenoliths (Canary Islands). Journal of Petrology, Special Lithosphere, 271–290.

Smith, D., Reiter, J.C.A., Mertzman, S.A., 1999. Water–rock interactions, orthopyroxene growth, and Si enrichment in the mantle: evidence in xenoliths from the Colorado Plateau, southwestern United States. Earth and Planetary Science Letters 167, 347–356.

Springer, R.K., 1974. Contact metamorphosed ultramafic rocks in the western Sierra Nevada foothills, California. Journal of Petrology 15, 160–196.

Stephens, C.J., 1997. Heterogeneity of oceanic peridotites from the western canyon wall at MARK: results from Site 920. In: Karson, J.A., Cannat, M., Miller, D.J., Elthon, D. (Eds.), Proceedings of the Ocean Drilling Program, Scientific Results, vol. 153, pp. 285–303.

Stillman, C.J., 1987. A Canary Islands dyke swarm: implications for the formation of oceanic islands by extensional fissural volcanism. In: Halls, J.M., Fahrig, W.F. (Eds.), Mafic Dyke Swarms, Geological Association of Canada, Special Paper, vol. 34, pp. 243–255.

Stillman, C.J., Fúster, J.M., Bennell-Baker, M.J., Muñoz, M., Smewing, J.D., Sagredo, J., 1975. Basal complex of Fuerteventura, (Canary Islands) is an oceanic intrusive complex with rift-system affinities. Nature 257, 469–471.

Suhr, G., Seck, H.A., Shimizu, N., Günther, D., Jenner, G., 1998. Infiltration of refractory melts into the lowermost oceanic crust: evidence from dunite- and gabbro-hosted clinopyroxenes in the Bay of Islands ophiolite. Contributions to Mineralogy and Petrology 131, 136–154.

Takahashi, N., 1992. Evidence for melt segregation towards fractures in the Horoman mantle peridotite complex. Nature 359, 52–55.

Trommsdorff, V., López Sánchez-Viscaíno, V., Gómez-Pgnaire, M.T., Müntener, O., 1998. High pressure breakdown of antigorite to spinifex-textured olivine and orthopyroxene, SE Spain. Contributions to Mineralogy and Petrology 132, 139–148.

Verhoef, J., Collette, B.J., Dañobeitia, J.J., Roeser, H.A., Roest, W.R., 1991. Magnetic anomalies off West-Africa (20–38°N). Marine Geophysical Research 13, 81–103.

Whitmarsh, R.B., Minshull, T.A., Russell, S.M., Dean, S.M., Louden, K.E., Chian, D., 2001. The role of syn-rift magmatism in the rift-to-drift evolution of the West Iberia continental margin: geophysical observations. In: Wilson, R.C.L., Whitmarsh, R.B., Taylor, B., Froitzheim, N. (Eds.), Non-Volcanic Rifting of Continental Margins: a Comparison of Evidence from Land and Sea, Geological Society, London, Special Publications, vol. 187, pp. 107–124.

Wilshire, H.G., 1987. A model of mantle metasomatism. In: Morris, E.M., Pasteris, J.D (Eds.), Mantle Metasomatism and Alkaline Magmatism, Geological Society of America, Special Paper, vol. 215, pp. 47–60.

Wilshire, H.G., Shervais, J.W., 1975. Al-augite and Cr-diopside ultamafic xenoliths in basaltic rocks from western United States. Physics and Chemistry of the Earth 9, 257–272.

Wilshire, H.G., Pike, J.E., Meyer, C.E., Schwarzman, E.L., 1980. Amphibole-rich veins in lherzolite xenoliths, Dish Hill and Deadman Lake, California. American Journal of Science 280A, 576–593.

Wulff-Pedersen, E., Neumann, E.-R., Jensen, J.J., 1996. The upper mantle under La Palma, Canary Islands: formation of Si–K–Na-rich melt and its importance as a metasomatic agent. Contribution to Mineralogy and Petrology 125, 113–139.

Yaxley, G.M., Green, D.H., Kamenetsky, V., 1998. Carbonatite metasomatism in the southeastern Australian lithosphere. Journal of Petrology 39, 1917–1930.